

# Shock Propagation Across the Futures Term Structure: Evidence from Crude Oil Prices

*Delphine H. Lautier,\* Franck Raynaud,\*\* and Michel A. Robe\*\*\**

---

## ABSTRACT

To what extent are futures prices interconnected across the maturity curve? Where in the term structure do price shocks originate, and which maturities do they reach? We propose a new approach, based on information theory, to study these cross-maturity linkages and the extent to which connectedness is impacted by market events. We introduce the concepts of backward and forward information flows, and propose a novel type of directed graph, to investigate the propagation of price shocks across the WTI term structure. Using daily data, we show that the mutual information shared by contracts with different maturities increases substantially starting in 2004, falls back sharply in 2011–2014, and recovers thereafter. Our findings point to a puzzling re-segmentation by maturity of the WTI market in 2012–2014. We document that, on average, short-dated futures emit more information than do backdated contracts. Importantly, however, we also show that significant amounts of information flow backwards along the maturity curve—almost always from intermediate maturities, but at times even from far-dated contracts. These backward flows are especially strong and far-reaching amid the 2007–2008 oil price boom/bust.

**Keywords:** Mutual information, Market integration, Information entropy, Shock propagation, Directed graphs, Term structure, Futures, Crude oil, WTI.

<https://doi.org/10.5547/01956574.40.3.dlau>

## 1. INTRODUCTION

Commodity futures markets fulfill the key economic functions of allowing for hedging and price discovery. In these markets, two important questions arise.

First, are futures prices interconnected across the maturity curve? In theory, they should be linked through the cost-of-carry relationship. In practice, such market integration requires cross-maturity arbitrage. Büyüksahin et al. (2009), however, document that even the three largest U.S. commodity futures markets did not witness substantial trading activity in longer-dated derivatives until 2003–2004 (crude oil) or later (corn and natural gas). This empirical fact suggests the possibility of changes in cross-maturity linkages in the past fifteen years.

Second, assuming that different-maturity futures prices are interconnected, where in the term structure do price shocks originate—and which other parts of the term structure do they reach? Is the direction of the shocks' propagation stable over time? A conventional view takes the physical

\* PSL Research University Paris Dauphine, CNRS UMR7088, DRM.

\*\* Department of Computational Biology, University of Lausanne (UNIL).

\*\*\* Corresponding author. College of ACES, University of Illinois at Urbana-Champaign. Send correspondence to Mumford Hall 334, University of Illinois at Urbana-Champaign, 1301 W Gregory Drive, Urbana, IL 61801, U.S.A. Email: [mrobe@illinois.edu](mailto:mrobe@illinois.edu).

market as the place where the absolute (or “flat”) price emerges as a function of the supply and demand for the underlying asset. In turn, the derivative market allows for relative pricing: futures prices derive from the spot price. Price shocks should thus spread from the underlying asset to the derivative instrument. Yet, amid a massive increase in far-dated commodity futures trading after 2003, might one not expect to also observe price shocks propagating from the far end to the short (physical) end of the futures curve?

There is, to our knowledge, no theoretical model studying these questions in a setting where multiple maturities of futures contracts trade simultaneously. In this paper, we investigate market integration and shock propagation empirically through the prism of the theory of information.

We introduce the concepts of “forward” and “backward” information flows across the term structure, and we rely on net transfer entropies to construct a novel type of directed graph linking all the parts of the term structure. Our laboratory is the New York Mercantile Exchange’s (NYMEX) market for West Texas Intermediate (WTI) light sweet crude oil futures. This market provides an ideal setting for our analysis: among all commodity markets in 2000–2017, WTI futures boast the highest level of trading activity and the greatest number of far-out delivery dates.

The theory of information, first outlined in a seminal paper by Shannon (1948), studies the measure, storage, and quantification of information. A key concept, in this theory, is “entropy”—the amount of uncertainty associated to a random variable. In our paper, the information entropy  $H(R_\tau)$  of the price return  $R$  on a crude oil futures contract of maturity  $\tau$  is a quantity that captures the degree of uncertainty associated to  $R_\tau$ . In other words,  $H(R_\tau)$  measures how much we don’t know about that oil futures’ price returns.

In this setting, we use the concept of “mutual information” to investigate futures market integration across maturities. When two variables are interdependent (as is the case, for example, for two time series of futures price returns with two different maturities), the mutual information measure gives the amount of entropy that is reduced (i.e., the amount of uncertainty that is resolved) compared to the case where the two variables are independent (Shannon and Weaver (1949); Schreiber (2000)). Computing the mutual information between contracts is thus analogous to assessing their integration or return co-movements. In contrast to other methods such as Pearson correlations, this probabilistic approach does not require making any assumption about the functional form of the relationship between the variables under consideration.

We find substantial variations over time in the amount of mutual information shared by crude oil futures with different delivery dates. In general, intermediate-maturity contracts (six months to two years) share relatively more mutual information than other contracts do. For all contracts, cross-maturity mutual information increases dramatically after 2003 (amid tight oil supply conditions, a dramatic growth in backdated crude oil futures trading, and the onset of commodity markets’ financialization) and reaches a peak at the top of the oil price boom in Summer 2008. It falls back sharply in 2012 (to pre-2005 levels) and drops further in 2013 and 2014 (to pre-2002 levels). It has since recovered dramatically. Taken together, these term-structure findings point to a puzzling re-segmentation by maturity of the WTI market in 2012–2014.

We also investigate the propagation of price shocks across the futures term structure, relying for this purpose on the concept of “transfer entropy” (Schreiber (2000)) that allows for dynamic analyses and for the determination of directionality. It enables us to answer the following question: does a shock to the price return of a futures contract with maturity  $\tau$  at time  $t$  beget a shock at time  $t+1$  to a futures contract with another maturity? Determining directions is important, as it allows us to ascertain whether price shocks evolve from short-term to long-term maturities or *vice versa*. Focusing on directionality relates our work to extant studies of Granger (1969) causality—but in a

non-parametric world. The technique can also be compared to the exploration of volatility spillovers (as in Adams and Glück (2015) or Jaeck and Lautier (2016)) while allowing for non-linearities—a crucial advantage given ample evidence that the dynamics of cross-market contagion (i.e., shock propagation) are non-linear.<sup>1</sup>

On average across our 2000–2017 sample period, we find that contracts with maturities up to 21 months emit more information entropy than do more backdated contracts—a pattern consistent with the traditional view of how futures market function. A dynamic analysis, however, reveals that the amount of entropy emitted by other parts of the curve is non-trivial and can be high at times. Moreover, the directions of the entropy transfers (from near-dated to far-dated contracts or *vice versa*) is not stable over time. In particular, an analysis of information entropy flows that run “forward” (i.e., from near-dated to further-out maturities) vs. “backward” (i.e., from backdated to nearer-dated contracts) shows that the backward flows are actually *higher* than their forward counterparts in 2008, i.e., during a 12-month period encompassing the peak of the 2007–2008 oil price boom and the subsequent price collapse after the Lehman crisis.

Finally, we utilize those non-parametric measures to define a metric that allows us to build an original type of directed graphs. The latter complement our other tests and provide a powerful visualization tool—as well as a means to detect anomalies—for our high-dimensional data. Indeed, insofar as all the futures prices that we study create a system, the latter is complex: it comprises many components that may interact in various ways through time. To wit, on any day in our sample, after discarding illiquid maturities, there remain 33 different WTI futures delivery dates: hence, we have 528 pairs of maturities to examine after accounting for directionality. Moreover, such linkages may change through time as a result of evolving market conditions or trading practices. Finally, chances are few that the relationships between different maturities are always linear.

A graph gives a representation of pairwise relationships within a collection of discrete entities. Each point of the graph constitutes a node (or vertex). In our analysis, a node corresponds to the time series of price returns on a futures contract for a given maturity over a specified period of time. The links (“edges”) of the graph can then be used in order to describe the relationships between nodes. More precisely, the graph can be weighted in order to take into account the intensities and/or the directions of the connections. We do both on the basis of information theory.

There are several ways to enrich the links of a graph. In the finance literature on commodity markets, for example, the connections between the nodes have been tied to the correlations of returns (e.g., Lautier and Raynaud (2012)), variance decompositions of return volatilities (Diebold et al. (2018)), or the activities of futures market participants (e.g., Adamic et al. (2017)). Here, we rely on the theory of information in order to determine the intensities of the links and to obtain their directions. To our knowledge, such an application is original in both the finance and commodity literatures.

The use of graph theory in this context allows us to examine precisely where the information entropy is transferred in the futures price system, and how far throughout the term structure it flows in practice. To that effect, we construct a reference graph that depicts the average behavior of the system in 2000–2017. In part, we find that this benchmark graph supports a conventional view of how a futures market operates—specifically, the notion that price shocks are thought to form in the physical market (here represented by the short maturities) and transmit to the paper market (here made up of further-out maturities). At the same time, however, we find that intermediate maturities send out substantial amounts of information entropy not only to further-dated contracts but also to near-dated ones. Furthermore, a dynamic analysis shows that there are sometimes major changes

1. See, e.g., Favero and Giavazzi (2002), Bekaert et al. (2014), Rigobon (2017), and references cited therein.

in the organization of the cross-maturities connections. The biggest such rearrangement is in Fall 2008, with the direction of information flows “flipping” entirely (i.e., originating at the far end of the curve and reaching even the shortest maturities). To the best of our knowledge, while this kind of reverse information-flow pattern is theoretically conceivable, our analysis provides the first empirical evidence of its existence.

Section 2 summarizes our contribution to the literature. Section 3 outlines our methodology, which is based on mutual information and transfer entropy. Section 4 presents the data. Section 5 summarizes our entropy findings. Section 6 is devoted to directed graphs. Section 7 concludes.

## 2. LITERATURE

We contribute to three literatures: on term structures and cross-maturities market segmentation, on causality, and on the use of graph theory in the context of financial and commodity markets.

Questions related to the impact of market imperfections on cross-maturities segmentation—defined as a situation in which different parts of the price term structure are disconnected from each other—date back to the works of Culbertson (1957) and Modigliani and Sutch (1966) regarding “preferred (maturity) habitats” in bond markets. Spurred by interest rate behaviors observed during the 2008–2011 financial crisis and the so-called Great Recession, the past ten years have seen a resurgence of theoretical and empirical work documenting increased bond market segmentation during periods of elevated market stress.<sup>2</sup> In commodity markets, research on possible cross-maturity segmentation across the futures term structure has to date remained purely empirical.<sup>3</sup> It deals almost exclusively with the crude oil market, which boasts high trading volumes and (in the United States) contract maturities extending up to seven years. In contrast to interest rate markets, extant papers find evidence of market segmentation prior to 2003 but conclude that the 2008–2011 financial crisis did not bring about a re-segmentation across maturities in the crude oil space.<sup>4</sup>

Our paper adds to this prior work in several ways—by quantifying the mutual information shared by contracts of different maturities, assessing the direction of the information entropy flows between maturities, and documenting how these measures evolve over time. Our analyses, while based on different techniques, are consistent with prior findings of increasing crude oil market integration through 2010. However, unlike the cross-maturity integration that characterized the 2004–2010 period, we document that different parts of the WTI term structure became much less integrated in 2011 and, especially, in 2012–2014. Furthermore, we find that changes in the degree

2. For example, D’Amico and King (2013) document the 2009 emergence of a “local supply” effect in the U.S. yield curve amid the Federal Reserve’s unprecedented program to purchase \$300bn worth of Treasury securities. Gürkaynak and Wright (2012), who review this literature, conclude that “the preferred habitat approach (has) value, especially at times of unusual financial market turmoil” (p. 360).

3. Theoretical work on the term structure of futures prices for commodities in general, and crude oil in particular, includes many distinguished contributions such as Schwartz (1997), Routledge et al. (2000), Casassus and Collin-Dufresne (2005), Casassus et al. (2018), Carlson et al. (2007), Kogan et al. (2009), Liu and Tang (2010), and Baker (2016). The models proposed in those papers, however, do not deal with the possibility that market frictions (e.g., limits to arbitrage or informational asymmetries) may prevent different parts of the futures price curve from moving in sync. A different part of the literature on commodity price formation analyzes the role of spot markets in revealing trader information. That body of work comprises theoretical work by Stein (1987) and Smith et al. (2015), as well as empirical work by Ederington et al. (2012) on crude oil. Those papers highlight the role of physical inventories. Instead, we investigate empirically how (and how much) information travels across the term structure of a large commodity futures market.

4. Based on the informational value of futures prices, Lautier (2005) finds cross-maturity segmentation during the 1990’s but argues that this market segmentation weakens after 2002. Using recursive cointegration techniques and term structure data from 1995–2011, Büyüksahin et al. (2011) find cointegrated WTI futures prices in 2003–2011.

of market integration are not always associated with similar changes in the respective intensities of the information entropy transfers that flow “forward” vs. “backward” across the term structure. In particular, we discover situations (most notably in 2007–2008) when backward flows actually (but atypically) become higher than their forward counterparts.

Finally, the present paper belongs to a growing literature that uses graph theory to investigate price connections across space and/or across markets for equities (e.g., Wang (2010); Dimpfl and Peter (2014)) and commodities (e.g., Haigh and Bessler (2004); Haigh et al. (2004); Lautier and Raynaud (2012); Diebold et al. (2018)). Compared with this body of work, our article innovates along two main dimensions.

First, at the technical level, we utilize another type of graph based on the theory of information. Building on mutual information and entropy transfers, our graph-based analyses allow us to study *all* the cross-maturity connections in the WTI futures market, within a non-parametric setting. Our methodological choice allows us also to deal with possible non-linearities and with the sheer size of the system we consider (528 daily pairs of futures maturities after accounting for directionality).

Second, while the spatial dimension of market integration has been analyzed in depth elsewhere for equities and currencies as well as for commodities, the time dimension has not. Most papers investigate the relationship between spot and futures prices<sup>5</sup> and simply abstract from term structure issues. A few papers do look at price integration across maturities (Lautier and Raynaud (2012); Büyüksahin et al. (2011)), but no prior study investigates the information entropy emitted (or received) by commodity futures of different maturities or the direction of the resulting information flows across a commodity term structure. Our paper does. We document for the first time that, while on average more information entropy flows forward than backwards, the backward flows are far from trivial, the intermediate maturities play an important informational role (sending entropy forward *and* backward), and the information entropy flows across the WTI term structure change not only in magnitude but also in direction during the “great oil price boom/bust” of 2007–2008.

### 3. METHODOLOGY

This Section presents several concepts for two series of futures price returns corresponding to a pair of contract maturities, which Section 5 will generalize in order to study the interdependence and directionality of price movements for multiple futures contracts. Throughout the paper, we rely on the theory of information based on the notions of entropy proposed by Shannon (1948). Section 3.1 presents the concept of “mutual information” (Shannon and Weaver (1949)) that quantifies the dependency between two random variables—which we use as a proxy for market integration. Unlike correlations, the mutual information measure captures non-linear relationships between variables; however, it does not allow for studying the propagation of information. For that purpose, Section 3.2 introduces the Schreiber (2000) transfer entropy measure.

5. In that context, a key empirical question is whether price discovery takes place on the futures or the spot market (Garbade and Silber (1983)). While early studies tend to rely on Granger causality to provide an answer, a number of papers apply other techniques in an attempt to tease out causality when the relationship between prices might be non-linear—see, e.g., Silvapulle and Moosa (1999), Switzer and El-Khoury (2010), Alzahrani et al. (2014) and references cited in those papers. Kawamoto and Hamori (2011) do look at WTI futures contracts with maturities up to nine months, but their focus is on market efficiency and unbiasedness—not on information flows.

### 3.1 Mutual information

In what follows, we consider a time series of price returns for a given futures maturity  $\tau$  as a discrete random variable  $R_\tau$  with an empirical probability distribution  $p(R_\tau)$ . We start from the interdependence of a pair of futures contracts. This measure of their interdependence, also called “mutual information,” relies on the use of several quantities: the “information entropy” of one variable, as well as the conditional and joint entropies of two variables. These different measures are linked to each other.

A first step is to consider the “information entropy”  $H(R_\tau)$  of the futures price return for a given maturity  $\tau$ . This quantity captures the degree of uncertainty associated to the variable  $R_\tau$ . In other words, it measures how much we don’t know about that price return.  $H(R_\tau)$  is maximized when all the possible realizations of  $R_\tau$  are equally likely.

Formally, following Shannon (1948), the information entropy  $H(R_\tau)$  associated to the futures prices’ returns for a given maturity  $\tau$  is defined as:

$$H(R_\tau) \equiv - \sum_r p(r_\tau) \log p(r_\tau) \quad (1)$$

where  $\sum_r$  is the sum over all the possible values of  $R_\tau$  and  $\log$  denotes the base 2 logarithm. Note that this quantity increases with the number of possible values for the random variable; for a binary random variable, its value ranges between 0 and 1—a fact that we shall exploit for the empirical analysis in Section 5.

Next, consider the case of two maturities  $\tau_1$  and  $\tau_2$ , and the interdependency between  $R_{\tau_1}$  and  $R_{\tau_2}$ . Let  $p(r_{\tau_1}, r_{\tau_2})$  denote the joint probability distribution of the two variables. What remains unknown of  $R_{\tau_1}$  if the values of  $R_{\tau_2}$  are known is captured by the notion of “conditional entropy,” i.e., the entropy of  $R_{\tau_1}$  conditionally on  $R_{\tau_2}$ :

$$H(R_{\tau_1} | R_{\tau_2}) \equiv - \sum_{r_{\tau_1}, r_{\tau_2}} p(r_{\tau_1}, r_{\tau_2}) \log \frac{p(r_{\tau_2})}{p(r_{\tau_1}, r_{\tau_2})} \quad (2)$$

Using the conditional probability distribution of the two variables  $p(r_{\tau_1} | r_{\tau_2})$ , Equation (2) becomes:

$$H(R_{\tau_1} | R_{\tau_2}) = - \sum_{r_{\tau_1}, r_{\tau_2}} p(r_{\tau_1}, r_{\tau_2}) \log p(r_{\tau_1} | r_{\tau_2}) \quad (3)$$

Another interesting quantity is the “joint information entropy”  $H(R_{\tau_1}, R_{\tau_2})$ . It quantifies the amount of information revealed by evaluating  $R_{\tau_1}$  and  $R_{\tau_2}$  simultaneously. This symmetric measure is related to the conditional entropy described by equations (2) and (3) as follows:

$$H(R_{\tau_1}, R_{\tau_2}) \equiv H(R_{\tau_1} | R_{\tau_2}) + H(R_{\tau_2}) = H(R_{\tau_2} | R_{\tau_1}) + H(R_{\tau_1}) \equiv H(R_{\tau_2}, R_{\tau_1}) \quad (4)$$

On the basis of these definitions, it is now possible to define the “mutual information”  $M(R_{\tau_2}, R_{\tau_1})$ . This quantity measures the amount of information obtained about one variable through the other. The mutual information  $M(R_{\tau_2}, R_{\tau_1})$  gives the amount of uncertainty that is reduced when two variables are *interdependent*, compared to the case where the two variables are *independent*:

$$M(R_{\tau_1}, R_{\tau_2}) \equiv H(R_{\tau_1}, R_{\tau_2}) - H(R_{\tau_1} | R_{\tau_2}) - H(R_{\tau_2} | R_{\tau_1}) = M(R_{\tau_2}, R_{\tau_1}) \quad (5)$$

The mutual information is thus a symmetric quantity. Equations (1), (2), and (5) together yield:

$$M(R_{\tau_1}, R_{\tau_2}) = \sum_{r_{\tau_1}, r_{\tau_2}} p(r_{\tau_1}, r_{\tau_2}) \log \frac{p(r_{\tau_1}, r_{\tau_2})}{p(r_{\tau_1})p(r_{\tau_2})} \quad (6)$$

In this article, we use mutual information as a measure of the integration of the crude oil futures market in the maturity dimension. This quantity indeed includes what would have been obtained with synchronous correlations between pairs of futures prices' returns, due to the common history of the returns and/or to common shocks. Compared with correlations, however, this probabilistic approach does not rely on any assumption regarding the behavior of futures returns.

### 3.2 Transfer entropy

To analyze the propagation of shocks along the futures term structure, we need to account for time lags and directions. We aim to answer the question: does a shock to the return of a given maturity  $\tau_2$  at time  $t-1$  induce a shock at time  $t$  to another maturity  $\tau_1$ ? Directions allow us to assess whether price shocks evolve from short-dated to long-dated contracts, or *vice versa*. This idea is closely linked to Granger causality, but in a non-parametric world. It is also related to volatility spillovers, except for the fact that it allows for non-linear interdependencies between variables.

Starting from the information entropy, a natural way to proceed is to rely on the notion of “transfer entropy” motivated and derived by Schreiber (2000). This measure quantifies how much information entropy (or uncertainty) is *transported* between dates  $t-1$  and  $t$  from one variable to another (in our case, from one futures maturity to another). It relies on transition probabilities rather than on static probabilities.

Relying on the definition of conditional entropy described by Equation (3), and introducing time into the analysis, allows for defining a new quantity: the “entropy rate”  $h$ . Two kinds of rates can be distinguished, according to the type of dependence under consideration. First, the entropy rate  $h_t(R_{\tau_1})$  quantifies the uncertainty on the next value of  $R_{\tau_1}$  if only the previous state of  $R_{\tau_1}$  matters:

$$h_t(R_{\tau_1}) = -\sum p(r_{\tau_1}^t, r_{\tau_1}^{t-1}) \log p(r_{\tau_1}^t | r_{\tau_1}^{t-1}) \quad (7)$$

Second, the entropy rate  $h_t(R_{\tau_1} | R_{\tau_2})$  quantifies the uncertainty on the next value of  $R_{\tau_1}$  if the previous states of  $R_{\tau_1}$  and  $R_{\tau_2}$  both have an influence:

$$h_t(R_{\tau_1} | R_{\tau_2}) = -\sum p(r_{\tau_1}^t, r_{\tau_1}^{t-1}, r_{\tau_2}^{t-1}) \log p(r_{\tau_1}^t | r_{\tau_1}^{t-1}, r_{\tau_2}^{t-1}) \quad (8)$$

With these dynamic measures defined, it is possible to introduce directions into the analysis. The “transfer entropy”  $T$  from  $R_{\tau_2}$  to  $R_{\tau_1}$  is the difference between the two rates:

$$T_{t, R_{\tau_2} \rightarrow R_{\tau_1}} = h_t(R_{\tau_1}) - h_t(R_{\tau_1} | R_{\tau_2}) = \sum p(r_{\tau_1}^t, r_{\tau_1}^{t-1}, r_{\tau_2}^{t-1}) \log \frac{p(r_{\tau_1}^t | r_{\tau_1}^{t-1}, r_{\tau_2}^{t-1})}{p(r_{\tau_1}^t | r_{\tau_1}^{t-1})} \quad (9)$$

This transfer entropy measure is equivalent to Granger causality in the case of a linear dependency between two Gaussian random variables—see Barnett et al. (2009). Compared to Granger causality, however, transfer entropy presents the major advantages of being model-free and of holding in the case of non-linearity.

Equipped with the above definitions, we can provide an insightful analysis of the propagation of price shocks along the term structure, for all maturity pairs and all directions. As needed, in

Section 5, we extend these pairwise concepts to the case of multiple maturities. Then, in Section 6, we utilize these concepts in the framework of graph theory.

#### 4. DATA

We obtain, from Datastream, the daily settlement prices for all NYMEX WTI light sweet crude oil futures contracts between January 2000 and January 2017. We roll futures based on prompt-contract expiration dates and construct 33 time series of futures prices. The first 28 are for the 28 nearest-dated contract maturities (i.e., contracts with 1 to 28 months until expiration). The other five time series correspond, respectively, to contract maturities of 30, 36, 48, 60, and 72 months.

Our empirical analyses use daily returns, computed as:  $r_{\tau} = (\ln F_{\tau}(t) - \ln F_{\tau}(t - \Delta t)) / \Delta t$ , where  $F_{\tau}(t)$  is the price of the futures contract with maturity  $\tau$  on day  $t$  and  $\Delta t$  is the time interval, measured in calendar days, between consecutive sample days (i.e., between business days).

Figure 1 depicts the evolution of WTI futures prices and price returns in our sample period. For readability, we focus on the nearby, one-year out, and two-year out futures. The right-hand side panel of Figure 1 shows that return volatility is lower for the two longer-dated contracts than for the nearby contract, an empirical reality consistent with the Samuelson (1965) hypothesis that price volatility should increase as a futures contract's maturity nears.<sup>6</sup>

**Figure 1: WTI Crude Oil Futures Prices and Daily Returns, 2000–2017**

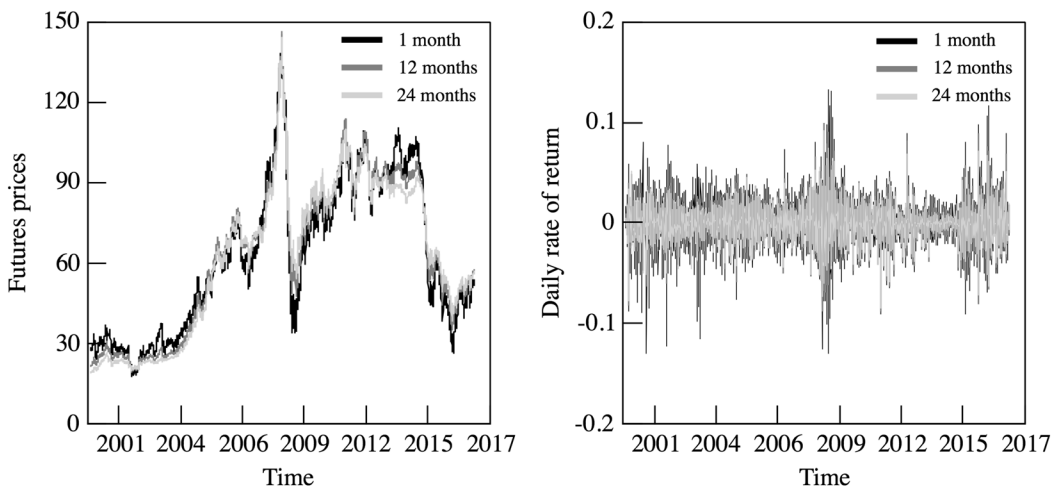


Figure 1 depicts the evolution of the daily prices levels of (left-hand side panel)—and the rates of return on fully collateralized positions in (right-hand side panel)—the nearby, one-year-out, and two-year-out West Texas Intermediate (WTI) light sweet crude oil futures in our sample period, i.e., from January 2000 to January 2017. We use the NYMEX end-of-day settlement prices in both panels (*Source*: Datastream). Futures roll dates are calendar-based.

Obvious in the left-hand side panel of Figure 1 are the oil price boom of 2004–2008 (peaking in mid-July 2008) and the consequent bust in Fall 2008. Equally notable, and especially relevant to the present study, are the differences between the price paths of nearby vs. longer-dated contracts prior to 2004 and again in 2012–2014. We know from prior research (Lautier (2005); Büyüksahin

6. We obtain the same volatility ranking when we use the preponderance of the open interest (rather than calendar dates) to determine futures roll days.



et al. (2011)) that the one-year (two-year) futures prices did not move in sync with the nearby price prior to 2003 (2004) but started doing so soon thereafter. Figure 1 confirms and extends those prior findings by showing that: i) starting in late 2012, a “disconnect” reappears between short-dated and further-dated WTI futures; ii) this disconnect, however, disappears after 2014.

## 5. EMPIRICAL RESULTS: ENTROPY MEASURES

Section 5.1 presents empirical evidence on the mutual information shared by crude oil futures with different maturities and on the evolution of this mutual information over time. Section 5.2 then introduces directionality and examines information entropy flows across the term structure of prices. Section 5.3 relates some of our findings to the Samuelson (1965) effect.

### 5.1 Mutual Information: A Proxy for Market Integration

Changes in the WTI futures market during the period under consideration can be characterized through the lens of mutual information. Recall from Section 3.1 that the mutual information measure quantifies how much we know about the return  $R_{\tau_1}$  given that the return  $R_{\tau_2}$  is known. In other words, this quantity captures the synchronous moves in prices. In what follows, we distinguish between the mutual information shared by all the futures contracts under consideration *vs.* the mutual information attached to one specific maturity.

#### 5.1.1 Mutual information shared by all maturities

On the basis of Equation (6), which defines the mutual information  $M_t(R_{\tau_1}, R_{\tau_2})$  for a pair of WTI futures maturities  $\tau_1$  and  $\tau_2$ , we define the average mutual information shared at date  $t$  by all  $N$  futures prices' returns,  $M_t^N$ , as follows:

$$M_t^N \equiv \langle M_t(R_{\tau_i}, R_{\tau_j}) \rangle_{i,j>i} \quad (10)$$

where: a)  $N$  is the total number of maturities each day in the sample; b) the  $M_t(R_{\tau_i}, R_{\tau_j})$  are the elements of the  $(N \times N)$  matrix of mutual information computed on day  $t$  using daily returns for the prior year;<sup>7</sup> c)  $\langle \rangle_{i,j>i}$  denotes the averaging operator over the relevant contract maturities ( $i = 1, 2, \dots, N$ ;  $i < j \leq N$ ).

Figure 2 depicts the dynamic behavior of  $M_t^N$  in 2000–2017 and establishes the statistical significance of our results. To assess significance, we start by generating a counterfactual dataset by “shuffling” (using permutations of) the time index of the original dataset (Marschinski and Kantz (2002)). The resulting “shuffled” time series of futures returns have the same mean and variance as the original ones, but temporal relationships are removed. Next, we compute the mutual information associated to the shuffled data. Figure 2 shows that, in contrast to the mutual information  $M_t^N$  associated with the original price series (plotted in black), the counterfactual mutual information

7. To obtain mutual information measures, we need to compute the joint and conditional entropies in Equation (5). We proceed as follows. For any futures price return  $R_t$ , we retain two possible states: either a positive or a negative value. In the case of a positive value, the number +1 is assigned to the observation; otherwise –1 is retained. We then empirically determine the probabilities  $p(1)$  and  $p(-1)$  associated to each maturity on a specific window of time. As we are interested in pairs of futures prices returns, for any pair there are four possible states: (1,1), (1,-1), (-1,1) and (-1,-1). When computing entropies, we therefore need a window that is long enough to have sufficiently many observations for each state. We set the window length at a year or 250 trading days (the results are qualitatively similar if we use 2-year rolling windows). Note finally that, as each element of the mutual information matrix analyzes a pair of variables and as we compute the conditional values on the basis of two states (a positive and a negative one), the highest possible value for the mutual information is 1: the results are normalized by the base 2 logarithm.

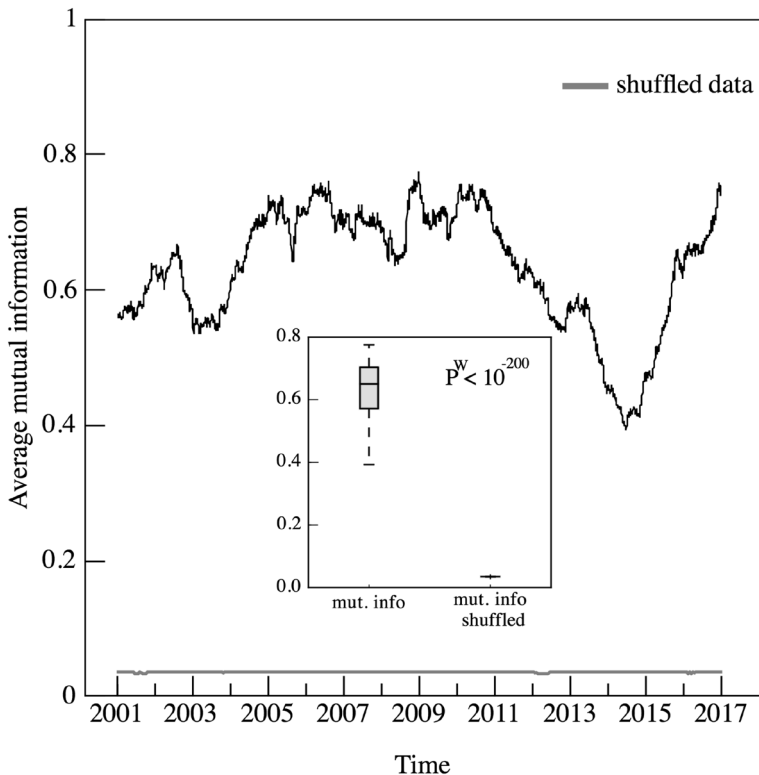
**Figure 2: Average Mutual Information  $M_t^N$  Shared Daily by All Maturities, 2001–2017**

Figure 2 plots in black the evolution over time of the average mutual information  $M_t^N$  shared at date  $t$  by all WTI futures contract maturities, from 2001 to 2017 (in our sample,  $N=33$  contracts each day). Daily values are first computed for each maturity using a one-year rolling window and then are averaged over all contract maturities. The scale is from 0 (no mutual information) to 1 (all futures price-return series are perfectly synchronized). The shuffled data (plotted as the medium-grey line toward the bottom of the graph) are counterfactual data created in order to perform statistical significance tests. To assess the significance of our results, we use a Welch's  $t$ -test. The associated results are depicted by the box within Figure 2. The  $p$ -values associated to the test are denoted by  $p^W$ . They give the probability that we cannot reject the null hypothesis that the average mutual information is the same, in the sample period, for the actual and shuffled data.

(plotted in medium grey, based on the shuffled series) is always close to 0 and does not display any systematic pattern over time. Finally, we establish that the actual and shuffled mutual information series are statistically significantly different using a Welch's  $t$ -test. It is an adaptation of the Student's  $t$ -test that is more reliable when the two samples under consideration do not have the same variance. The associated  $p$ -values, denoted by  $p^W$  in Figure 2, give the probability that the null hypothesis cannot be rejected. As these probabilities are very low, the results can be considered as significant.

Figure 2 establishes two important empirical facts. First, the mutual information shared by all maturities starts to rise sharply in 2004 and takes very high values from mid-2004 through most of 2010:  $M_t^N$  generally fluctuates between 0.7 and 0.75, vs. a theoretical maximum of 1 (see footnote 7). These high values are evidence of synchronization in the prices changes across maturities.<sup>8</sup> Insofar as an increase in  $M_t^N$  can be interpreted in terms of greater integration of the futures market

8. In this sense, the mutual information can be compared with the co-movements captured by a Principal Component Analysis (PCA). More precisely, an analysis of the returns of commodity prices shows that the first factor extracted through the PCA represents parallel moves in the term structure. It can thus be associated to the co-movement in prices (see, e.g., Cortazar and Schwartz (1994)). In our 2000–2017 dataset, the first factor of the PCA explains more than 95% of the variability

for crude oil during that period, this first result complements and extends to many more maturities a key finding of Büyüksahin et al. (2011), based on 1983–2010 data, that the nearby, one-year out, and two-year out WTI futures prices are statistically significantly cointegrated starting in mid-2004.

Second, Figure 2 shows that  $M_t^N$  starts to decrease sharply after December 2010, before falling even more precipitously in 2013–2014 (reaching its 2000–2017 minimum of 0.39 in June 2014). This finding is novel. It provides formal support for our interpretation of the price patterns depicted by Figure 1 and discussed in Section 4: in 2013 and 2014, different parts of the term structure of WTI futures prices became (temporarily) much less integrated.

A natural question is what explains this temporary re-segmentation of the WTI market across futures delivery dates. Büyüksahin et al. (2011) attribute the WTI futures market’s cross-maturity integration in 2004–2010 in large part to huge increases in far-dated futures trading and in calendar-spread trading by hedge funds and other financial institutions, amid what has been dubbed the “financialization of commodities” (Cheng and Xiong (2014)). On the one hand, as those authors’ dataset ends in mid-2010, their trading-related findings might seem irrelevant to the behavior of the mutual information after 2010. On the other hand, financialization did *not* end in 2010: public data from the U.S. Commodity Futures Trading Commission (CFTC) on weekly WTI futures trader positions show that both the WTI non-commercial open interest and calendar spread trading continued to *increase* from 2010 through 2014—suggesting that a different explanation, unrelated to the levels of non-commercial futures trading, may have to be found for the evolution of  $M_t^N$  in 2011–2014.<sup>9</sup>

Interestingly, the decrease of  $M_t^N$  seen in Figure 2 starts at the very end of 2010 and comes to a halt in late 2014. Those four years coincide almost exactly with a period of exceptionally high levels of the Brent-WTI price spread amid a partial geographic segmentation of the world’s crude oil markets—events that Büyüksahin et al. (2013) link to a temporary divergence between crude supply-side conditions in North America vs. in the rest of the world.<sup>10</sup> Our findings thus point to the need for further research in order to assess the extent to which those physical market developments had implications that went beyond commodity price spreads and that reached into the amount of mutual information shared across the WTI term structure.

### 5.1.2 Mutual information for each contract maturity

Figure 3 gives more insight into the term structure developments detected in Figure 2, by depicting the mutual information for each individual contract maturity over the course of our sample period. Precisely, for each futures maturity  $\tau_i$  and each day of the sample period  $t$ , Figure 3 plots the level of mutual information that this maturity shares with all other maturities:

$$M_t(R_{\tau_i}) = \langle M_t(R_{\tau_i}, R_{\tau_j}) \rangle_{j, j \neq i}$$

This level is color-coded in Figure 3, ranging from dark grey (low) to light grey (high).

In general, Figure 3 shows that not all futures prices have the same levels of mutual information. Strikingly, at any given time in our sample period, there is much more mutual information at the intermediate maturities (defined as contracts expiring in 6 to 27 months): contracts at both

of WTI futures returns and displays a very high correlation (+0.69) with our measure of mutual information. These results are available from the authors upon request.

9. Fully ruling out trading-related explanations would require disaggregated CFTC data, which are not publicly available.

10. Fattouh (2010), Pirrong (2010), and Büyüksahin et al. (2013) also analyze a less severe episode of Brent-WTI price dislocation in 2008–2009 that was due largely to infrastructure constraints at the delivery point for WTI futures in Cushing, OK. Those infrastructure issues had been mostly ( *completely*) resolved by 2011 (2013–2014).

**Figure 3: Mutual Information Shared Daily by Each Maturity with All Other Maturities, 2001–2017**

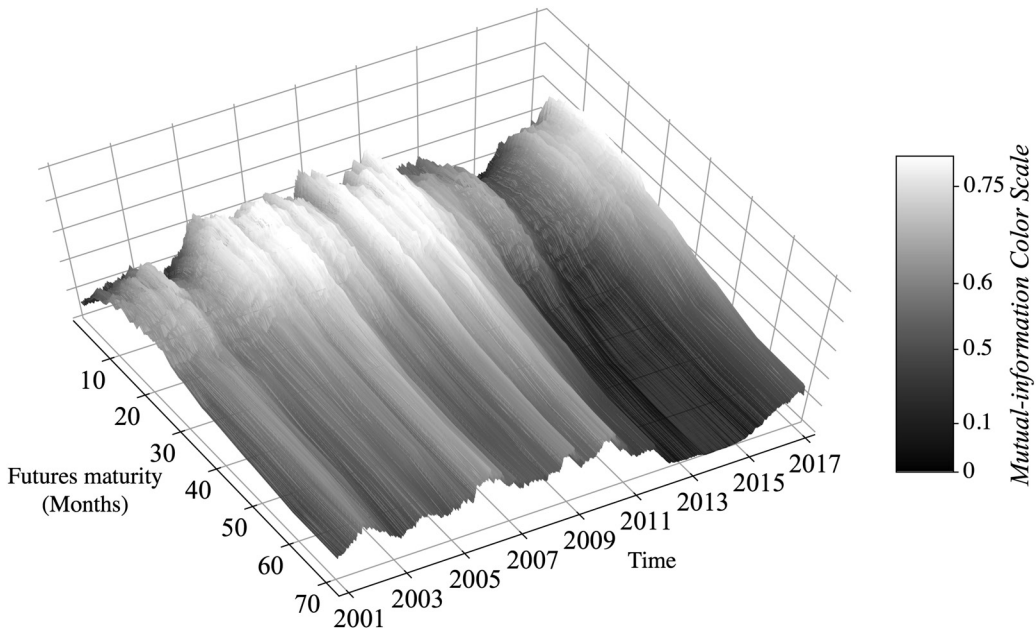


Figure 3 depicts the mutual information shared by each maturity with all other maturities over the course of our 2000–2017 sample period. For every maturity  $i=1,2,\dots,72$  and every business day in 2001–2017, the level of mutual information that this maturity shares with all others is computed using daily returns for the previous 250 trading days and is displayed using a grey scale ranging from dark grey (very low mutual information) to light grey (very high mutual information). We chose a non-linear color gradation to improve readability of the figure in grey-scale.

extremities of the futures maturity curve share less mutual information with other contracts than the intermediate-maturity ones do. Furthermore, except for the last five months of 2008 and in 2012–2014, the graph temperature is typically darker at the very short end of the term structure (plotted at the top of the graph) than at the far end of the curve (at the bottom of the same graph), indicating that the nearest-dated contracts usually contain the least mutual information. This finding is consistent with the notion that short-dated crude oil futures prices are more volatile—sending more information and thus sharing less mutual information.<sup>11</sup> Overall, these results suggest that the WTI futures term structure consists of three main segments: from the 1st to the 3rd months, from the 4th to the 27th months, and finally the most distant delivery dates (contracts maturing in 30 months and beyond).

Figure 3 also documents that, as a rule across the universe of maturities, the mutual information i) is much higher in 2004–2011 than in 2001–2003 and (especially) than in 2012–2014, and ii) returns to this very high level after 2015. The middle part of the maturity curve, where the amount of mutual information is the highest, is also fatter in 2004–2011 than in the three years before or after. In other words, Figure 3 establishes that the market integration phenomenon observed in Figure 2 comes principally from what happens at intermediate maturities.<sup>12</sup>

11. See Robe and Wallen (2016) for recent evidence on the term structure of WTI implied volatilities.

12. Figure 4 complements Figures 2 (mutual information over time, across all maturities) and 3 (mutual information over time for each individual maturity) by depicting the information that a specific maturity shares *on average* with all other maturities in 2000–2017. It shows that the average mutual information is a hump-shaped function of contract maturity, with

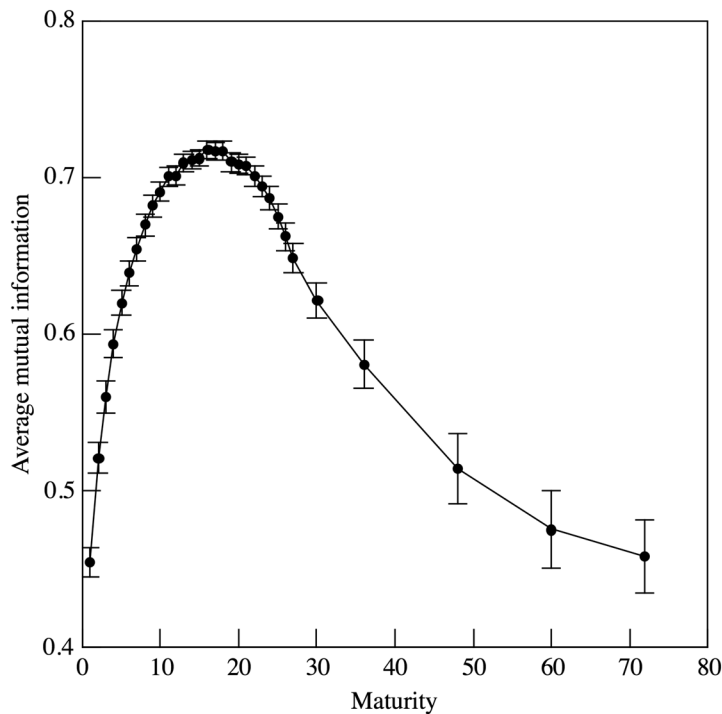
**Figure 4: Average Mutual Information Shared by Each Maturity with All Others, 2001–2017**

Figure 4 represents the information that a specific WTI futures maturity (in months) shares, on average between January 2001 and 2017, with all other maturities. Daily values are computed using settlement prices and a one-year rolling window using contract price data from 2000–2017, and then are averaged for each maturity over the 2001–2017 period. The bars around each point show the average variance of the measure over the sample period.

Finally, we know from Figure 2 that an important market development took place in 2011–2014, with the total mutual information  $M_t^N$  falling after December 2010 and reaching record low levels in 2014. Figure 3 shows that, while the graph gets darker across the *entire* spectrum of maturities during that period, the maturities that darken the most are the most backdated ones (contracts with maturities greater than three years).

## 5.2 Transfer Entropy between Maturities

This Section investigates cross-maturity linkages through the lens of the entropy transfers between contract maturities. It adds to the insights already gained from the mutual information analyses in Section 5.1 by answering the question of which part of the term structure is the shock transmitter and which one is the receiver. We first perform a static analysis across the whole sample period (Section 5.2.1), and then carry out dynamic analyses in order to assess how the typical emission and reception patterns evolve over time (Section 5.2.2). Finally, we define and compute “backward” and “forward” information flows across the term structure (Section 5.2.3).

a maximum near the 18-month maturity. It also confirms that the intermediate maturities (6 to 27 months) share substantially more mutual information than contracts both at the back end of the curve (shown up to 6 years out) and at the front end—especially the nearby contract.

### 5.2.1 Static analysis: Sample-average transfer entropies associated to each maturity

We start by computing the transfer entropies over the entire sample period. This approach gives us a picture of the “average” behavior of the system, i.e., it shows whether one maturity sends on average more than what it receives or *vice-versa*. Starting from Equation (9), which focuses on the transfers between two maturities  $\tau_1$  and  $\tau_2$ , we extend this pairwise measure and compute—for every trading day  $t$  in our sample—the total amount of entropy sent from the futures prices’ return with maturity  $\tau_i$  to all other maturities  $\tau_j$  ( $j \neq i$ ):

$$T_{i,R_{\tau_i}}^S = \sum_{j \neq i} T_{i,R_{\tau_i} \rightarrow R_{\tau_j}} \quad (11)$$

Similarly, we define the daily quantity received by maturity  $i$  from all the other maturities as:

$$T_{i,R_{\tau_i}}^R = \sum_{j \neq i} T_{i,R_{\tau_i} \leftarrow R_{\tau_j}} \quad (12)$$

Figure 5 depicts the daily transfer entropies associated to each WTI futures maturity, averaged over all trading days in our sample period. The black line in the figure shows the total amount of information entropy emitted by each maturity, using 2000–2017 averages of the daily values computed using Equation (11). The grey line shows the total amount of information entropy received by each contract, based on Equation (12). The vertical bars in the figure represent, for each maturity, the average sample variance recorded for the specific measure; these variances are particularly large for the entropy received by the long-dated contracts.

**Figure 5: Average Daily Total Transfer Entropies by Maturity, 2001–2017**

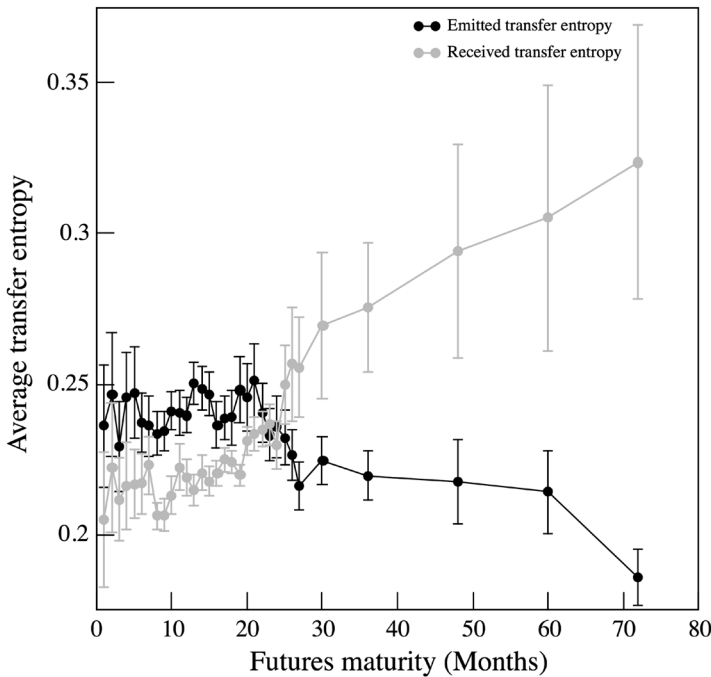


Figure 5 depicts time-averages of the daily transfer entropies that are emitted (black line) or received (grey line) by each maturity. Daily values of the total transfer entropies emitted or received are computed for each maturity using equations (11) or (12), using a one-year rolling window of WTI futures prices from 2000–2017, and then are averaged over the 2001–2017 period. The bars around each point show, for each maturity, the variance recorded for the measure over the sample period.

Figure 5 shows that, on average, maturities up to two years (including the 24-month contract) emit more than they receive. For contract maturities beyond 24 months, the average information entropy emitted by a contract is decreasing in its maturity—with an especially sharp drop at 60 months. The average information entropy received exhibits the opposite pattern: it is lowest for the first 24 maturities and highest for maturities of 25+ months (with the maximum value reached at the back end of the term structure). Intuitively, these static results imply that crude oil market participants whose “preferred habitat” (Modigliani and Sutch (1966)) is the back end of the maturity curve are, on average, more likely to be the object of a shock than to be the source of one.

### 5.2.2 Dynamic analysis: Transfer entropies over time, by maturity

For each maturity  $\tau_i$  and every trading day  $t$  in 2000–2017, Figure 6 plots the total entropy  $T_{t,R\tau_i}^S$  sent from  $\tau_i$  to all the other maturities. Figure 7 plots  $T_{t,R\tau_i}^R$ , the total entropy received by  $\tau_i$  from all the other maturities.

Together, these two 3-D plots show that the short (1–3 months) and/or intermediate maturities (6–27 months) send out the most information entropy (see Figure 6) while the longer maturities (30+ months) are those that receive the entropy (see Figure 7). As such, for much of 2000–2017, the daily entropy transfer patterns match the average (“static”) pattern of Figure 5 discussed in Section 5.2.1.

Figures 6 and 7, however, also show that those typical patterns are turned on their head between mid-2007 and early Fall 2008. Very large transfer entropies start being sent by futures with

**Figure 6: Daily Transfer Entropy Emitted by Each Maturity to All Other Maturities, 2001–2017**

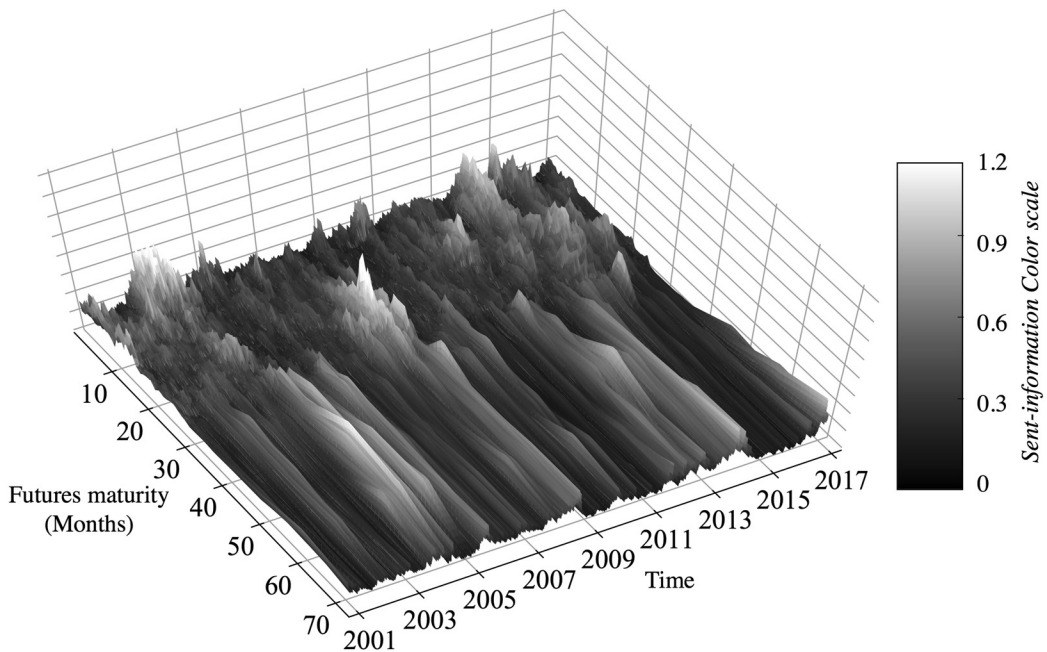


Figure 6 shows the transfer entropy emitted by each WTI futures maturity to all other contract maturities on each trading day in our sample. Daily values of the total transfer entropies emitted are computed for each maturity using Equation (11), using a one-year rolling window of WTI futures prices from 2000–2017. The entropy emitted is displayed in a color ranging from blue (very low) to green, yellow, orange or red (very high).

**Figure 7: Daily Transfer Entropy Received by Each Maturity from All Other Maturities, 2001–2017**

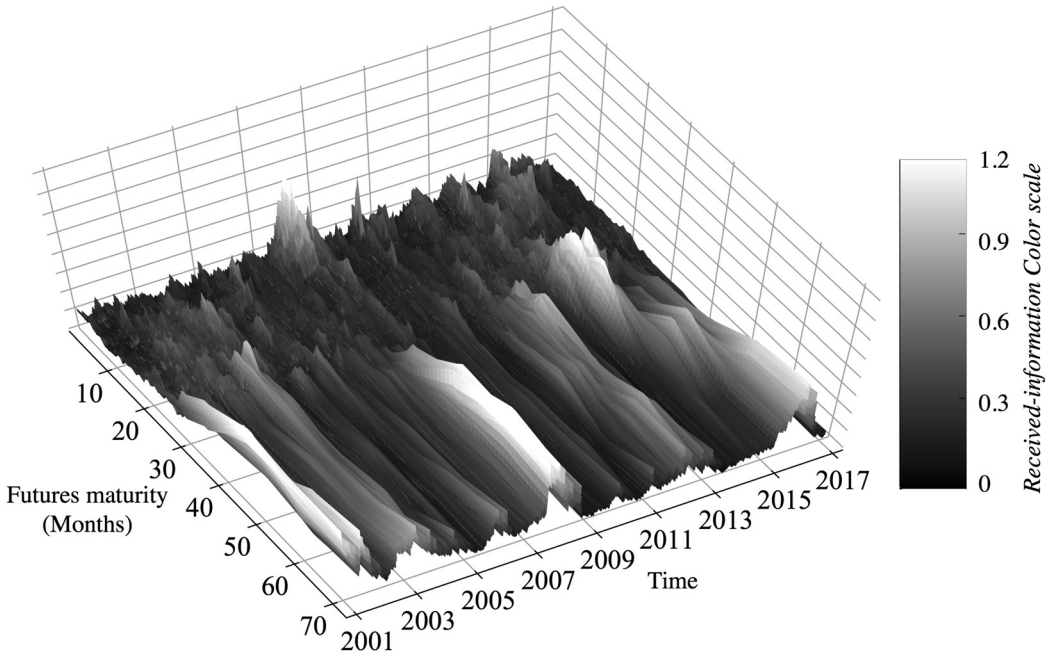


Figure 7 shows the transfer entropy received by each WTI futures maturity from all other contract maturities, for every day in our sample period. Daily values of the total transfer entropies received are computed for each maturity using Equation (12), using a one-year rolling window of WTI futures prices from 2000–2017. The entropy received is displayed in a color ranging from blue (very low) to green, yellow, orange or red (very high).

maturities from 12 to 27 months (it is the only time when those maturities appear in light or very light grey in Figure 6).

At the same time, not only the long-dated contracts (as is typical) *but also* the nearest-dated futures (which is *atypical*) become the recipients of exceptionally large transfer entropies (see Figure 7). For the three nearest-dated contracts, the differences between the entropies received and sent are much larger (especially between July 2007 and July 2008) than at all other times in 2000–2017: in essence, the nearby, first- and second-deferred contracts turn almost silent for much of that year.

As shown in Figure 1, this episode coincides with the oil price “boom/bust of 2007–2008”—see, e.g., Singleton (2014). It is truly exceptional: at no other time in the sample period do the nearest-dated contracts receive so much information entropy nor do the intermediate maturities send out as much entropy. As such, the 2007–2008 period deserves more attention: we therefore explore it further, using directed graphs, in Sections 6.3 and 6.4.

### 5.2.3 Forward and Backward Information Flows

The transfer measure  $T_{R_{t_i}}^S$  [*resp.*  $T_{R_{t_i}}^R$ ] defined by Equation (11) [*resp.* Equation (12)] captures the total entropy sent [*resp.* received] by a single maturity, no matter the direction of this emission [*resp.* the origin of this reception]. However, if we want to gain insights into the direction in which price shocks propagate, then we need to restrict the analysis to what is emitted in a single direction only, from *any* maturity.



To this end, we propose the notions of “forward” and “backward” information flows. We define the daily “forward flow” of information,  $\phi^F$ , as the sum across maturities of the transfers of entropy from *each* maturity  $\tau_i$  to *all further-out* maturities  $\tau_j$ :

$$\phi_t^F = \sum_{i=1}^N \sum_{j>i} T_{i,R_{\tau_i} \rightarrow R_{\tau_j}} \tag{13}$$

where  $\sum_{j>i}$  denotes summations over all the maturities greater than  $i$ . The “backward flow”  $\phi^B$  is defined analogously as:

$$\phi_t^B = \sum_{i=1}^N \sum_{j<i} T_{i,R_{\tau_i} \rightarrow R_{\tau_j}} \tag{14}$$

On any given day, the forward (*backward*) flow captures the propagation of price shocks in the direction of longer-dated (*shorter-dated*) futures.

The top panel of Figure 8 plots the forward and backward flows (graphed, respectively, in black and in dark grey) computed, using a rolling 1-year window, for each trading day from January 2001 to January 2017. The bottom-left panel of the same figure is devoted to significance tests on those information flows. Relying on the methodology developed for the mutual information, it shows that the flows associated to real data are statistically significantly different from those associated with counterfactual data where the time index has been randomly shuffled.<sup>13</sup>

Figure 8’s top panel delineates three main sub-periods in our sample. In almost all of 2000–2003 and much of 2014–2017 (“Sub-periods I and III” in Figure 8), the forward flows are higher than the backward flows: in economic terms, the term structure of WTI futures prices is generally more prone to influence from shocks arising at the near-end of the maturity curve. From 2004 through the Winter of 2014 (“Sub-period II”), in contrast, the amplitudes of the two information flows are generally similar: in other words, the driving forces of price movements are broadly equal all along the term structure, with price shocks propagating in the backward direction as easily as in the backward direction. Figure 8 even highlights a year in Sub-period II (namely, 2008) when the backward flows are not only exceptionally high but are, in fact, much stronger than the contemporaneous forward flows. This period, which includes the peak of the oil price boom (in the first half of 2008) and the subsequent crude price collapse (in the late Summer and Fall of 2008), is the same outlier that we already detected—using other information measures—in Sections 5.1.1 and 5.2.2.

A natural question is whether the relative strengths of forward vs. backward flows are statistically significantly different across sub-periods. The bottom-right panel in Figure 8 answers in the affirmative by analyzing the *difference* between forward and backward flows,  $\delta_{f-b}$ . The panel depicts the densities of distribution of  $\delta_{f-b}$  in each sub-period. Sub-period I, shown in black, is clearly characterized by higher forward flows. This is also the case for sub-period III (in green), which exhibits a bi-modal distribution. Sub-period II (in red), in contrast, is centered around null values. The same panel also provides the results of Kolmogorov-Smirnov (KS) tests. The notations  $p_{I-II}^{KS}$  correspond to the p-values of a KS test comparing the distribution of  $\delta_{f-b}$  in sub-period I with that of  $\delta_{f-b}$  in sub-period II. The probability that these two distributions are the same is extremely low. The same conclusion obtains for  $p_{II-III}^{KS}$  and  $p_{I-III}^{KS}$ .

13. We generate counterfactual forward- and backward-flow measures by “shuffling” the time index of each dataset. The resulting forward information flows are shown in medium grey (“Forward shuffled” in the figure) and the backward flows are in light grey (“Backward shuffled”). Unlike the actual forward and backward flows (depicted in black and dark grey, respectively), the counterfactual information flows fluctuate little. Crucially, their values are almost equal for all  $t$ .

Figure 8: Daily Forward and Backward Information Flows Between Maturities, 2001–2017

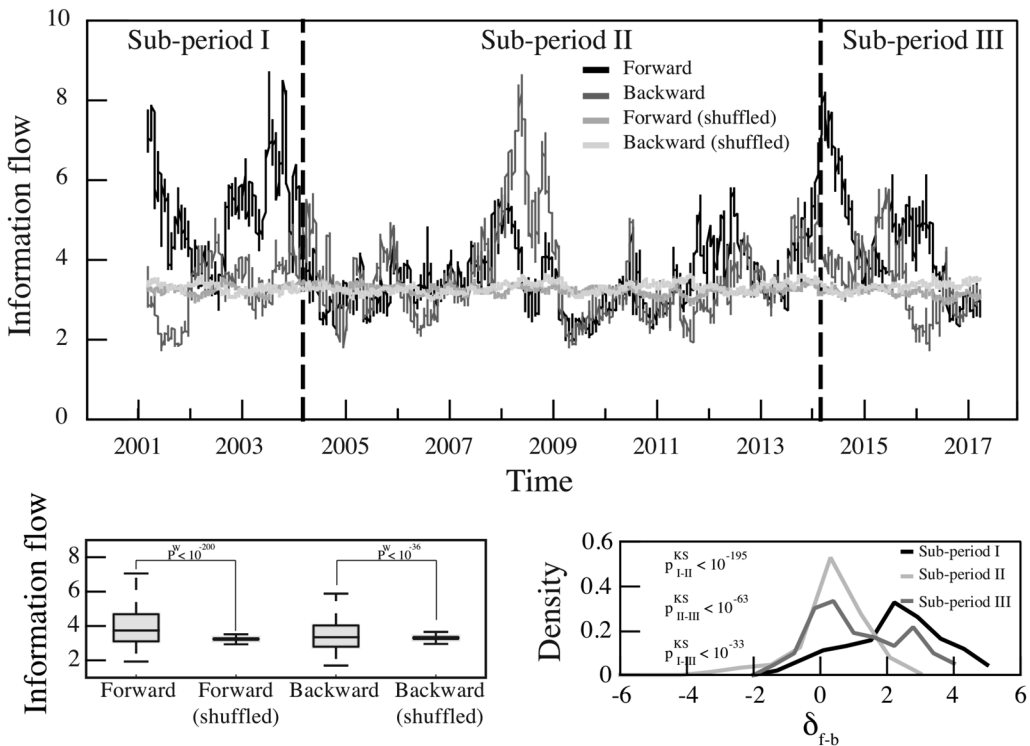


Figure 8 exhibits the daily information flows between WTI futures maturities in 2001–2017. The **top panel** illustrates the daily sum of information flows that are emitted by all maturities in the direction of longer maturities (“Forward”, black curve) and the daily sum of information flows received by all maturities from shorter maturities (“Backward”, dark grey curve). To provide a test for the statistical significance associated to these flows, we generate two counterfactual series—“Forward (shuffled)” and “Backward (shuffled)” —by using permutations of the time index of the underlying WTI futures price returns. These counterfactuals are plotted in medium grey (Forward) and light grey (Backward) in the top panel. The **second panel, on the bottom left**, gives the results of a Welch  $t$ -test that compares the information flows in the real data with those in the counterfactual data. The associated  $p$ -values are denoted by  $p^w$ . The **third panel, on the bottom right**, gives insights in the *difference* between the forward and the backward flows,  $\delta_{f-b}$ . It depicts the density of distribution of  $\delta_{f-b}$ .  $p_{A-B}^{KS}$  is the  $p$ -value of a Kolmogorov-Smirnov test comparing the distribution of  $\delta_{f-b}$  in sub-period  $A$  with that of  $\delta_{f-b}$  in sub-period  $B$ .

### 5.3 Discussion: Links with the Samuelson Effect

Our findings on forward and backward information flows raise questions regarding the so-called Samuelson effect. Samuelson (1965) hypothesizes that futures price volatility increases as the contract approaches expiration. Some theoretical models explain that effect.<sup>14</sup> Other models, though, predict that futures price volatility may instead decrease as expiration nears.<sup>15</sup>

Extant theoretical papers’ results on the Samuelson effect have direct implications for the relative volatility of futures with different maturities. Taken as a whole, they show that it is possible

14. Bessembinder et al. (1996), for example, identify conditions under which the Samuelson effect holds—such as asset markets in which spot price changes include a temporary component (so that investors expect mean-reversion). Note that a number of reduced-form term structure models generate a Samuelson effect without modeling it.

15. Anderson and Danthine (1983), for instance, show that “volatility may increase or decrease as delivery approaches depending upon the pattern of information flow into the market (*ibid.*, p. 257). Hong (2000) shows that the volatility-maturity relationship changes depending on whether market participants are symmetrically informed.

for the futures price volatility to be either increasing or decreasing across the term structure. Insofar as price volatility is related to the arrival of information, it might be tempting to conclude that the same models also predict that information could flow either forward or backward across the futures curve depending on circumstances—a possibility that Figure 8 establishes as an empirical fact.

In those models, however, a single futures contract trades at any point in time, and this contract moves closer to maturity each period—ruling out the possibility that information could flow in both directions across the term structure. We are not aware of any theoretical model that predicts a key informational role for intermediate maturities (Section 5.2.2), or why backward flows would dominate on 37 percent of all trading days in 2000–2017 (Section 5.2.3). In fact there is, to our knowledge, no model studying how market participants reveal information during price formation in a setting where multiple maturities of futures contracts trade simultaneously. Our empirical findings point to the need for such theoretical research.

Our results show that, in practice, there are price shocks coming from the far end of the crude oil futures term structure that spread to shorter maturities, and *vice versa*. An important question is how far they travel—in particular, are shocks at the far end of the futures curve strong enough to spread to the nearby contract and, thus, to the physical market? Section 6 answers this question.

## 6. DIRECTED GRAPHS

In this Section, we bring the non-parametric transfer entropy measures of Section 5.2.1 into the framework of graph theory, which is ideal for large-scale analyses. This innovation allows us to carry out an analysis of price shock transmission for *all* maturity pairs (528 daily links in our case).

We propose a directed graph that shows not only the directions of the pairwise transfer entropies, but also their strength, based on the net amount of entropy transported between two maturities (Section 6.1). We then use data from the entire sample to compute a benchmark graph representative of the average functioning of the market (Section 6.2). Next, we develop a measure of the “distance” between this sample-average graph and the graphs that we compute, using a one-year rolling window, for every day in 2000–2017. We find that, while the information flows across the term structure do generally follow the patterns seen in the benchmark graph, there are exceptions. From Fall 2004 to Fall 2005, and again from Fall 2007 to Winter 2009 (a period that includes the 2007–2008 oil price boom/bust, Lehman Brothers’ bankruptcy, and physical infrastructure issues affecting WTI futures), the cross-maturity information flows differ substantially from the benchmark case (Section 6.3). Finally, we conclude with a case study of the differences between the graph computed for the most “pathological” day in 2008–2009 (October 8, 2008) and the benchmark graph (Section 6.4).

### 6.1 Building Graphs using Transfer Entropy

A graph is defined by its nodes and links (or “edges”). We assign to each node the time series of price returns for a specific futures maturity. In our case, a graph thus has  $N = 33$  nodes.

In order to enrich the links of the graph regarding the direction and the intensity of the net transfer entropy between each given pair of nodes  $\tau_i$  ( $i = 1, \dots, N$ ) and  $\tau_j$  ( $j \neq i$ ), we define a daily “directionality index”  $D_{i,R_{\tau_i} R_{\tau_j}}$  as follows:

$$D_{i,R_{\tau_i} R_{\tau_j}} = \frac{T_{i,R_{\tau_i} \rightarrow R_{\tau_j}} - T_{i,R_{\tau_j} \rightarrow R_{\tau_i}}}{T_{i,R_{\tau_i} \rightarrow R_{\tau_j}} + T_{i,R_{\tau_j} \rightarrow R_{\tau_i}}} \quad (15)$$

The value of the index  $D_{t,R_{\tau_i},R_{\tau_j}}$ , which is bounded by  $-1$  and  $1$ , expresses the *strength* of the link between the maturities  $\tau_i$  and  $\tau_j$ .<sup>16</sup> Its sign gives the *direction* of the net entropy transfer: from  $R_{\tau_i}$  to  $R_{\tau_j}$  when  $D_{t,R_{\tau_i},R_{\tau_j}} > 0$ , and from  $R_{\tau_j}$  to  $R_{\tau_i}$  otherwise.

## 6.2 The Benchmark: The Sample-Average Directed Graph

To create a benchmark directed graph for the WTI futures market, we compute sample-average directionality indices. Based on Equation (9), we start by using one-year rolling windows to compute the transfer entropies  $T_{t,R_{\tau_i} \rightarrow R_{\tau_j}}$  from each contract maturity  $\tau_i$  to each other maturity  $\tau_j$ , for every trading day. Next, we average those daily values across our 2000–2017 sample. Finally, we input those  $N(N-1) = 1,056$  averages into Equation (15). This process yields 528 average directionality indices, which we denote  $\bar{D}_{R_{\tau_i},R_{\tau_j}}$  ( $i = 1, \dots, N; j \neq i$ ).

### 6.2.1 Capturing the graph's rich content

The resulting benchmark graph, with its dozens of nodes and hundreds of links, is very difficult to read. To make its interpretation easier, we filter it according to the strength of the connections between its nodes. Figure 9 depicts four filtered benchmark graphs, ranked in order of increasing link intensity  $\bar{D}$ . For example, the top-left panel focuses on the benchmark graph's weakest links:  $|\bar{D}_{R_{\tau_i},R_{\tau_j}}| < 0.25$ ; the top-right panel only shows links with  $0.25 \leq |\bar{D}_{R_{\tau_i},R_{\tau_j}}| < 0.5$ ; etc.

In addition to the intensity of the graph's links, it is useful to also keep track of the number of indegrees (*outdegrees*) at each of its nodes—that is, the number of nodes from which (*to which*) a given node receives (*sends*) net transfer entropy. A node's number of indegrees in Figure 9 is readily seen by counting, across the four panels, the arrows reaching that node. In order to simultaneously depict the average number of outdegrees from each node while preserving readability, we color-code the nodes from light grey (few outdegrees) to dark grey (many outdegrees). At each node, across the four panels, indegrees and outdegrees together sum up to  $N - 1 = 32$ .

### 6.2.2 Findings

The most obvious stylized fact in Figure 9 is that the links between maturity pairs are concentrated in the bottom two panels: put differently, on a typical day in 2000–2017, the information-related strength of most cross-maturity linkages is high. Figure 9 also shows where, on average, the information entropy flows from and where it flows to.

We already know from Figures 5 to 7 that far-dated WTI futures typically send little information but receive information from the rest of the term structure. Figure 9 refines this finding by showing that, in net terms, long-dated futures receive a lot of entropy from many different other maturities (lots of arrows hit nodes 30 through 72, and the vast majority of those arrows are seen in the bottom two panels where  $|\bar{D}| \geq 0.5$ ) and, conversely, are net senders of entropy to very few other maturities (these same nodes' colors are shaded in light grey in all four panels). Figure 9 tells us more than Figures 5 to 7, by showing that some of the information reaching the longest maturities comes all the way from the nearest-dated contracts. To wit, the bottom-left (*top-right*) panel shows high (*moderate*) net transfer entropies from the nearby, first-deferred, and second-deferred contracts

16. We define the normalized quantity  $D_{t,R_{\tau_i},R_{\tau_j}}$  to capture the strength of the directionality, rather than the quantity of information transmitted (on which Section 5.2 focuses instead). A variant of Equation (15), using its denominator's maximum across contracts, would capture the latter quantity.

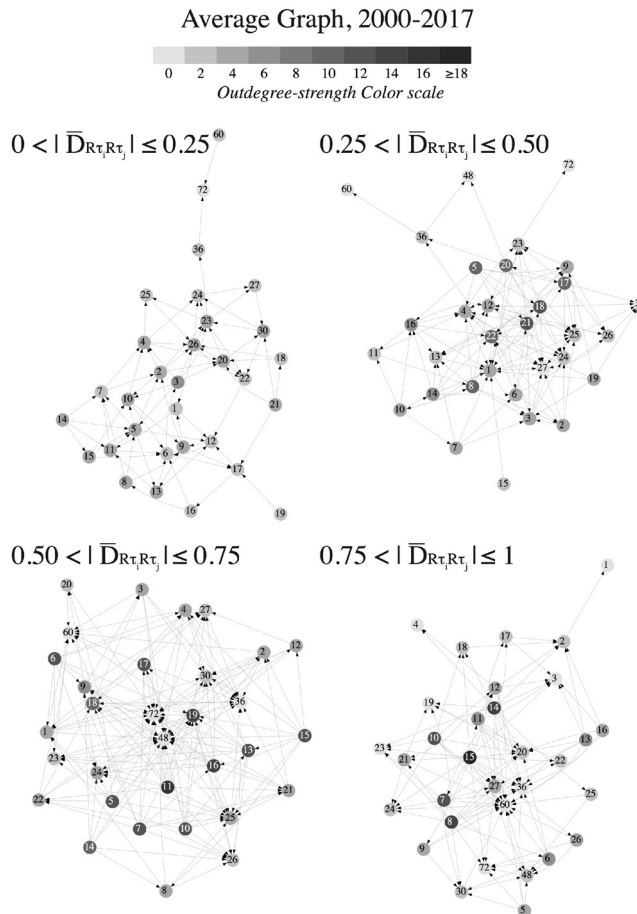
**Figure 9: Typical Filtered Directed Graph**

Figure 9 shows the net transfer entropies between WTI futures maturities between January 2000 and January 2017. Each node represents a time series of price returns for a given maturity; the maturity is denoted inside the node. The link between each pair of nodes is oriented according to the directionality index  $\bar{D}_{R_{\tau_i}, R_{\tau_j}}$ , i.e., the average net transfer entropy (15) between maturities  $\tau_i$  and  $\tau_j$ . The entire directed graph has 33 nodes and 528 links. For clarity, the graph is filtered—each panel displays only a subset of links. For example, the panel at the top left shows only the links with  $|\bar{D}_{R_{\tau_i}, R_{\tau_j}}| \leq 0.25$ . The color of each node in a graph reflects the number of arrows of a given index strength that go out of that node in direction of other nodes (i.e., “outdegrees”).

to all futures maturities between 30 and 72 months (*24 to 29 months*). In that sense, the benchmark directed graph appears to support a conventional view of how a futures market operates—specifically that price shocks are thought to form in the physical market (here represented by the short maturities) and transmit to the paper market (here made up of contracts with maturities of two years or more).

We also know from Figures 5 to 7, though, that many middle maturities (5 to 21 months) emit more entropy than they receive. Figure 9 goes beyond that finding by showing that those substantial net transfer entropies from middle maturities flow not only to further-out maturities but also to the shorter-dated futures. As a matter of fact, the biggest recipient of entropy from the middle of the term structure is the front-month contract (top-right panel in Figure 9). This finding calls for new theoretical work that would generate such a role for the intermediate maturities in a commodity futures market.

### 6.3 Dynamic Analysis: Daily Distance from the Benchmark Case

The directionality index also allows for dynamic analyses. On the basis of one-year rolling windows, we compute, at each date  $t$ , the instantaneous directionality matrix  $D_{t,R_{\tau_i}R_{\tau_j}}$ . This lets us construct daily directed graphs, whose properties and evolution over time we can examine. An important point of interest regarding the properties of daily directed graphs is their stability: do the directions in the graph evolve during the period? If so, then how?

To answer these questions, we start from the benchmark case (the sample-average directed graph built on the basis of the matrix of directionality  $\bar{D}_{R_{\tau_i}R_{\tau_j}}$ ) and measure the distance between that benchmark graph and the daily directed graphs. Our distance metric is the “survival ratio” or the proportion of links that retain the same direction in both graphs (Onnela (2003)). Here, we compute the daily average survival ratio  $\overline{SR}_t$  between the benchmark and daily graphs as:

$$\overline{SR}_t = \frac{2}{N(N-1)} \sum_{i=1}^N \sum_{j \neq i} I_{D_{t,R_{\tau_i}R_{\tau_j}} \cap \bar{D}_{R_{\tau_i}R_{\tau_j}}} \quad (16)$$

where the averaging is across maturities, and  $I_{D_{t,R_{\tau_i}R_{\tau_j}} \cap \bar{D}_{R_{\tau_i}R_{\tau_j}}}$  is an indicator function that takes the value 1 if  $D_{t,R_{\tau_i}R_{\tau_j}}$  has the same sign as  $\bar{D}_{R_{\tau_i}R_{\tau_j}}$  and 0 otherwise. On day  $t$ ,  $\overline{SR}_t$  quantifies the stability of the graph’s directionality: it tallies up the edges with the same directions in both graphs, and expresses that sum as a proportion of the total number of elements in each graph,  $N \frac{(N-1)}{2}$ . If  $\overline{SR}_t = 1$ , then the two graphs are identical in the sense that all the edges in both graphs have the same directions. At the other extreme, if  $\overline{SR}_t = 0$ , then the set of directed links is totally different.

The top panel of Figure 10 shows the distance between the benchmark graph and each of the daily graphs, measured through the time series of the survival ratios  $\overline{SR}_t$ . The daily survival ratio fluctuates between a maximum of 76% and a minimum of 24%; two thirds of the time, it is higher than 50%. This pattern indicates that in our sample period, day after day, a majority of the directed links are in the same state as in the benchmark case. The panel, however, also highlights two periods when the information flows change massively. The first such episode starts in late Fall 2004 and ends approximately a year later. The second episode, during which  $\overline{SR}_t$  reaches its lowest sample value, starts in mid-2008 and ends in Spring 2009.

In order to connect these two episodes with physical and futures market developments, we use the bottom panel of Figure 10. It reveals the maturities most affected by any reorganization of the graph. On a given day  $t$ , each maturity  $\tau_i$  is color-coded based on its survival ratio that day (ranging from dark grey for the lowest values, to light grey for the highest values). Precisely, we compute and plot  $SR_{t,\tau_i}$  ( $i = 1, \dots, N$ ):

$$SR_{t,\tau_i} = \frac{1}{N-1} \sum_{j \neq i} I_{D_{t,R_{\tau_i}R_{\tau_j}} \cap \bar{D}_{R_{\tau_i}R_{\tau_j}}} \quad (17)$$

During the first episode (2004–2005), Figure 10’s bottom panel pinpoints the far-out maturities as contributing the most to the graph’s reorganization—i.e., to the change in the pattern of shock propagation. It complements Figure 6 which shows that, during that period, futures of 2+ years send out uncharacteristically large amounts of information (for the first time ever). Interestingly, this very period witnessed a profound change in WTI trading activity, with open interest in WTI futures with maturities of 3+ years quadrupling compared to 2003 levels amid the financial-

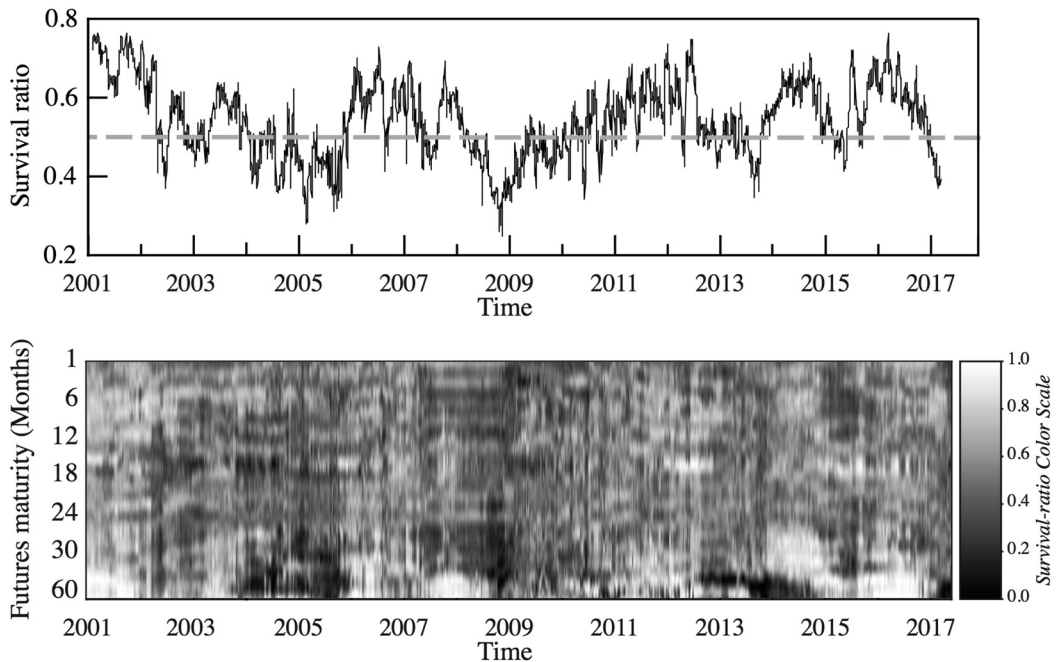
**Figure 10: Survival Ratios**

Figure 10 comprises two panels. The **top panel** provides insight into the distance between the static non-filtered directed graph, used as a benchmark, and daily directed graphs, by plotting the survival ratio  $\bar{S}_R(t)$ . We measure  $\bar{S}_R(t)$  as the number of same-sign elements in  $\frac{1}{N}D_{R_1, R_2}(t) \cap \bar{D}_{R_1, R_2}$ . For each day  $t$  from January 2001 to January 2017, the values are computed using daily returns from the prior year (a rolling window of 250 trading days). At one extreme, if  $\bar{S}_R(t) = 1$ , then the two graphs are identical—from which one concludes that the pattern of shock propagation has remained stable. At the other extreme, if  $\bar{S}_R(t) = 0$ , then the set of directed links has been completely rearranged (compared to the benchmark graph). In addition to the top panel's level of the survival ratios, the **bottom panel** identifies the individual maturities touched by the daily reorganization of the graph. Every day in the sample, each maturity is plotted on a grey-scale depending on whether the survival ratio is high (*light grey*) or low (*dark grey*).

ization of commodity markets (Büyüksahin et al. (2011)). Thus, our findings point to the need for a theoretical model in order to assess the extent to which financialization could bring about this kind of changes in cross-maturity informational linkages. During the second episode (2008–2009), the bottom panel of Figure 10 shows that, while long maturities contribute to the graph reorganization, so do the near-dated contracts—but only in the Fall of 2008 and Winter of 2009. Interestingly, that period starts with the demise of Lehman Brothers and continues with a massive steepening of the WTI futures curve amid a petroleum storage-capacity crisis at the WTI futures delivery point in Cushing, Oklahoma—see Büyüksahin et al. (2013). Once again, the methodology we have proposed is able to capture the impact of these market developments on information flows across the term structure.

#### 6.4 A Case Study: October 8, 2008

Figure 10's top panel shows that the survival ratio  $\bar{S}_R$  hits its two lowest values for the 2000–2017 period in Fall 2008. The first (26%) is reached on September 18—three days after Lehman Brothers' bankruptcy, two days after AIG's takeover by the U.S. Federal Reserve, and one day

**Figure 11: Filtered Directed Graph on October 8, 2008**

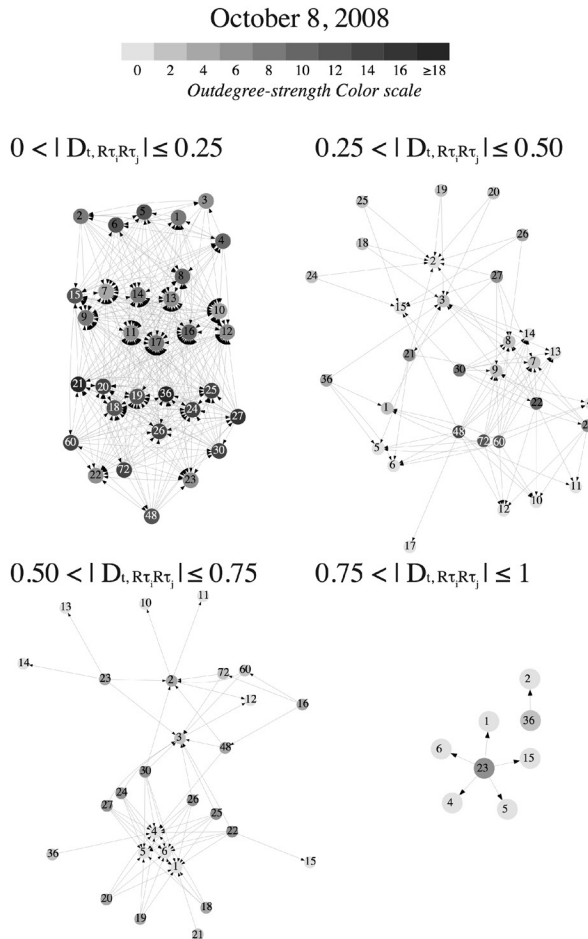


Figure 11 summarizes the net transfer entropies between WTI futures maturities on October 8, 2008. The link between each pair of nodes is oriented according to the directionality index  $D_{R_{\tau_i},R_{\tau_j}}$ , i.e., the net transfer entropy (15) between maturities  $\tau_i$  and  $\tau_j$ , computed using daily returns in the previous year. The entire directed graph has 33 nodes and 528 links. For clarity, the graph is filtered—each panel displays only a subset of links. For example, the panel at the top left shows only the links with  $|D_{t,R_{\tau_i},R_{\tau_j}}| \leq 0.25$ . The color of each node reflects the number of arrows of a given index strength that go out of that node in direction of other nodes (i.e., “outdegrees”).

after the rescue of HBOS (the UK’s then largest mortgage lender) by Lloyds. The other (24%) is reached three weeks later, on October 8, “amid the worst ever week for the Dow Jones.”<sup>17</sup>

Figure 11 provides the filtered graphs for a case study of the information flows across the WTI term structure on October 8, 2008. It is organized and color-coded exactly like Figure 9, allowing for easy comparisons with the sample-average directed graph. As such, several stylized facts emerge.

First, in Figure 11, most of the links are in the top left panel—where  $|D_{Oct8,R_{\tau_i},R_{\tau_j}}| \leq 0.25$  (Section 6.2.2). In Figure 9, in contrast,  $|\bar{D}_{t,R_{\tau_i},R_{\tau_j}}| \geq 0.5$  for most links.<sup>18</sup> In plain English, not only is the *direction* of the net information entropy transfer different from its sample-average for more

17. The Guardian (<https://www.theguardian.com/business/2012/aug/07/credit-crunch-boom-bust-timeline>).

18. Figure 12 provides two histograms of the link strengths in, respectively, Figures 9 and 11.



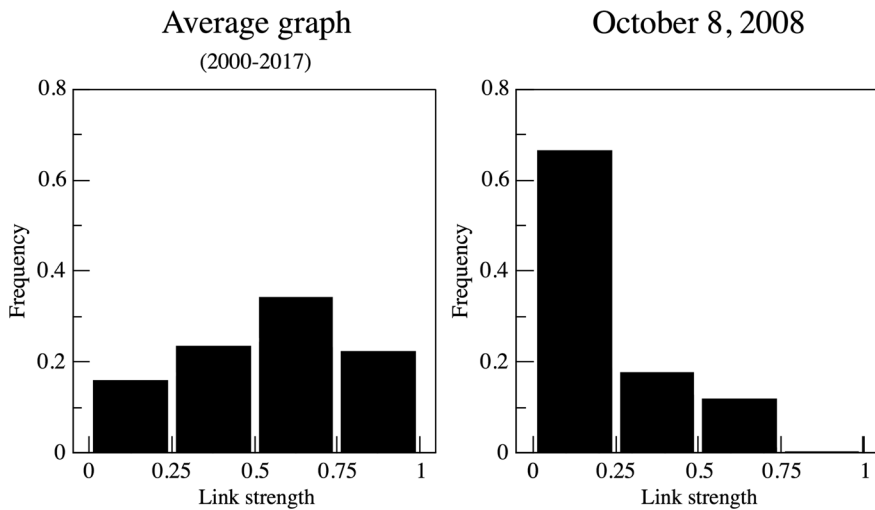
**Figure 12: Link Strength Frequency: Average Directed Graphs versus October 8, 2008**

Figure 12 compares the distribution of the 528 directionality indices  $D_{R_{\tau_i} R_{\tau_j}}$  (the net transfer entropies between WTI futures maturities  $\tau_i$  and  $\tau_j$ ) in Figure 9 (sample-average graph) vs. in Figure 11 (October 8, 2008 graph). Both directed graphs have  $N = 33$  nodes (one per maturity) and  $N(N - 1) = 528$  links between its nodes.

than three quarters of the 528 maturity pairs ( $\overline{SR}_{Oct.8} = 0.24$ ), but the *strength* of most of the pairwise directionality indices is also lower on October 8, 2008, than during much of 2000–2017.

Second, we know from Figure 5 that, on average, far-dated futures (30+ months) send little entropy to other maturities while receiving substantial amounts of entropy from those other maturities (Section 5.2.1). Furthermore, we know from Figure 9 that far-dated futures are net entropy recipients from virtually all the other maturities—including from the nearest-dated contracts (Section 6.2.2). We also know from Figures 6 and 7, however, that these patterns are turned on their head in 2008—with the front months becoming the recipients of very large transfer entropies (Section 5.2.2). What Figure 11 tells us—but the other figures could not reveal—is that, three weeks after Lehman’s collapse and amid a massive crude oil price plunge, the pattern is completely reversed:

- In the average graph, the only nodes that send net entropy to many other nodes (color code: medium to dark grey) correspond to maturities between 8 and 19 months. On October 8th, in contrast, the contracts that are similarly color-coded have maturities of 21+ months. Indeed, almost all of the nodes for futures of 21+ months are in medium to (very) dark grey.
- On October 8th, all the far-dated contracts are net senders of entropy to most other maturities, *including* the nearest-dated ones. To wit, the 6-year futures (node 72) hits the nearby with a medium-strength net transfer (top-right panel of Figure 11), and it hits the first-deferred with a high net transfer (bottom-left panel of Figure 11).

The graph computed for October 8, 2008, is based on a one-year rolling-window of returns. Hence, the fact that the lowest value of  $\overline{SR}_t$  is reached on October 8, 2008, implies that the entire prior year—corresponding to the oil price boom/bust of 2007–2008—is characterized by highly unusual information flows across the term structure. The extant literature on the financialization of commodities focuses on the impact of index traders’ and hedge funds’ trading activities on spot or nearby-futures prices, including the possibility that they may cause bubbles—see, e.g., Singleton

(2014) and Sockin and Xiong (2015). Our case study's findings suggest that other components of the futures curve, as well as the informational relationships between them, may be impacted too.

## 7. CONCLUSION

We apply the notions of mutual information and transfer entropy to investigate empirically the nature of pricing relationships across the WTI crude oil futures term structure in 2000–2017. In this setting, information refers to the uncertainty associated to a variable. It captures unexpected changes, typically a shock in the futures prices' return.

We use the level of mutual information across maturities as a proxy for market integration, and we introduce the notions of forward (*backward*) information entropy flows as proxies for the extent to which price shocks propagate in the direction of longer (*shorter*) maturities. Our forward and backward flows are conceptually related to volatility spillovers, but they allow for non-linear interdependencies between variables and for the analysis of a high-dimensional system (here, a term structure over two decades). We further innovate by proposing a novel type of directed graph linking different parts of the futures curve based on the net entropy transfers between maturity pairs.

First, we find major variations over time in the amount of mutual information shared between futures with different delivery dates. The mutual information increases substantially starting after 2003, falls back sharply in 2011–2014, and rises again thereafter. Büyüksahin et al. (2011), in a widely-cited study, show that the prices of the nearby, one-year, and two-year WTI futures became cointegrated in 2003–2010 due to a combination of tight supply conditions in the physical oil market and of commodity markets' financialization. Our findings point to a puzzling re-segmentation of the WTI market by maturity in 2012–2014. Further research, using regulatory trader-level activity data, is therefore needed to determine whether the 2011–2014 free-fall in mutual information levels can be explained by physical-market developments (perhaps those that brought about a concomitant surge of the Brent-WTI price spread) or, alternatively, by a possible pullback of key financial institutions from participation at the back end of the WTI futures curve (perhaps due to the anticipation, and the coming into force, of costlier regulatory requirements during that same period).

Second, our findings on the magnitude and direction of information entropy flows also suggests interesting venues for theoretical research.

On the one hand, we document that the short- and medium-dated futures are on average net senders of information entropy, and that they emit more entropy than longer-dated contracts do (30+ months). We also show that, on average, information entropy flows forward rather than backward—with price shocks transmitted all the way from the front to the far end of the futures curve. These facts appear consistent with a conventional view of how futures markets work: price shocks propagate in the forward direction.

On the other hand, we document for the first time that the intermediate maturities (6 to 24 months) play an important informational role, sending information forward *and* backward, and that the information flows change in magnitude *and* in direction amid the “oil price boom/bust” of 2007–2008. We even find that substantial *net* information transfers flow from the far end all the way to the very front end of the term structure during that boom/bust episode.

New theoretical models are needed to rationalize those findings and provide guidance on identification. While existing models of the Samuelson (1965) effect allow one to make predictions regarding the relative volatility of futures contracts with different maturities, all of them assume that only one futures contract trades at any given time. As such, those models are by construction unable to generate the bi-directional information flows across the term structure that our analysis reveals.

Doing so requires a micro-founded dynamic equilibrium model in which multiple futures maturities trade simultaneously.

Finally, our findings point to a number of new venues for empirical work. i) On the finance side, the methodology we propose in this paper could be applied to other markets, like financial futures. ii) It also raises tantalizing possibilities of applications in the realm of return predictability. iii) On the commodities side, a debate has raged for over a decade on the extent to which financialization is responsible for the 2007–2008 commodity price boom. Extant bubble studies focus on the spot or nearby futures prices. Our finding that the three nearest-dated WTI futures turn almost silent during that entire episode and, instead of emitting information, start receiving net entropy transfers from even the furthest-out contracts, indicates that any analysis of the 2007–2008 boom/bust must consider the possible impact of financialization on *all* the components of a term structure—not just its front end. iv) The past twelve years have witnessed numerous failures of U.S. agricultural futures and spot prices to converge at expiration, spawning a growing body of work analyzing this phenomenon (see, e.g., Garcia et al. (2015)). In that literature also, the focus is solely on the behavior of the spot and front-month futures prices. Extending the methodologies utilized in the present paper would make it possible to highlight the impact on the entire futures curve. Hence, it would allow for the development of a pathology of price discovery impairments and cross-maturity information-flow disruptions during such episodes—which would be of use to market participants, regulators, and futures exchanges.

## ACKNOWLEDGMENTS

We thank three referees for very helpful comments that have substantially improved the paper. We also thank Steve Baker, Scott Mixon, Teresa Serra, Casey Petroff, Steve Kane, Andrei Kirilenko, Patrice Poncet, and participants in seminars at the U.S. Department of Energy's (DOE) Energy Information Administration (EIA), the U.S. Commodity Futures Trading Commission (CFTC), the Finance for Energy Markets Research Initiative Lab (FiME, Institut Henri Poincaré, Paris), and the University of Illinois at Urbana-Champaign, and at the International Forum on Financial Risks (IFFR, Institut Louis Bachelier, Paris) and the 2017 AFFI International Conference (Valence, France) for useful suggestions. We thank Gautier Boucher, Pierre-Alain Reigeron, and Jonathan Wallen for research assistance. Lautier and Raynaud gratefully acknowledge support from the Finance and Sustainable Development Chair, and from the FiME and MIMO Research Initiatives. Raynaud also acknowledges the financial support of the Gabriella Giorgi-Cavaglieri Foundation. Robe gratefully acknowledges the financial support received in his capacity as The Clearing Corporation Foundation Professor in Derivatives Trading at the University of Illinois. Robe contributed to this project in a period during which he also consulted for the DOE and the CFTC. No compensation was received from, and no resources were used at, either the DOE or the CFTC for this project. The opinions expressed in this paper are the authors' only—not those of the DOE, the CFTC, or the U.S. government. Errors and omissions, if any, are the authors' sole responsibility.

## REFERENCES

- Adamic, L., C. Brunetti, J.H. Harris and A. Kirilenko (2017). "Trading Networks." *Econometrics Journal* 20(3):S126–S149. <https://doi.org/10.1111/ectj.12090>.
- Adams, Z. and T. Glück (2015). "Financialization in Commodity Markets: A Passing Trend or the New Normal?" *Journal of Banking and Finance* 60: 93–111. <https://doi.org/10.1016/j.jbankfin.2015.07.008>.
- Alzahrani, M., M. Masih and O. Al-Titi (2014). "Linear and Non-linear Granger Causality between Oil Spot and Futures Prices: A Wavelet Based Test." *Journal of International Money and Finance* 48(A): 175–201.

- Anderson, R.W. and J.-P. Danthine (1983). "The Time Pattern of Hedging and the Volatility of Futures Prices." *Review of Economic Studies* 50(2): 249–266. <https://doi.org/10.2307/2297415>.
- Baker, S.D. (2016). "The Financialization of Storable Commodities." *Working Paper*, University of Virginia, November 2012. Updated, March.
- Barnett, L., A.B. Barrett and A.K. Seth (2009). "Granger Causality and Transfer Entropy Are Equivalent for Gaussian Variables." *Physical Review Letters* 103: 238701. <https://doi.org/10.1103/PhysRevLett.103.238701>.
- Bekaert, G., M. Ehrmann, M. Fratzscher and A. Mehl (2014). "The Global Crisis and Equity Market Contagion." *Journal of Finance* 69(6): 2597–2649. <https://doi.org/10.1111/jofi.12203>.
- Bessembinder, H., J.F. Coughenour, P.J. Seguin and M.M. Smoller (1996). "Is There a Term Structure of Futures Volatilities? Reevaluating the Samuelson Hypothesis." *Journal of Derivatives* 4(2): 45–58. <https://doi.org/10.3905/jod.1996.407967>.
- Büyükhahin, B., M.S. Haigh, J.H. Harris, J.A. Overdahl and M.A. Robe (2011). "Fundamentals, Trading Activity and Crude Oil Pricing." *CFTC Research Paper* 2011-5, U.S. Commodity Futures Trading Commission, May.
- Büyükhahin, B., J.H. Harris, J.A. Overdahl and M.A. Robe (2009). "The Changing Structure of Energy Futures Markets." *Finance et Valeurs*, A. Corhay, G. Hübner and A. Müller Eds., ULG Press, Liège, Belgium.
- Büyükhahin, B., T.K. Lee, J.T. Moser and M.A. Robe (2013). "Physical Markets, Paper Markets and the WTI-Brent Spread." *Energy Journal* 34(3): 129–151.
- Carlson, M., Z. Khokher and S.S. Titman (2007). "Equilibrium Exhaustible Resource Price Dynamics." *Journal of Finance* 62(4): 1663–1703. <https://doi.org/10.1111/j.1540-6261.2007.01254.x>.
- Casassus, J., and P. Collin-Dufresne (2005). "Stochastic Convenience Yield Implied from Commodity Futures and Interest Rates." *Journal of Finance* 60(5): 2283–2331. <https://doi.org/10.1111/j.1540-6261.2005.00799.x>.
- Casassus, J., P. Collin-Dufresne and B.R. Routledge (2018). "Equilibrium Commodity Prices with Irreversible Investment and Non-linear Technologies." *Journal of Banking and Finance* 95: 128–147. <https://doi.org/10.1016/j.jbankfin.2018.04.001>.
- Cheng, I.-H. and W. Xiong (2014). "The Financialization of Commodity Markets." *Annual Review of Financial Economics* 6: 419–441. <https://doi.org/10.1146/annurev-financial-110613-034432>.
- Cortazar, G. and E.S. Schwartz (1994). "The Valuation of Commodity Contingent Claims." *The Journal of Derivatives* 1(4): 27–39. <https://doi.org/10.3905/jod.1994.407896>.
- Cortazar, G. and E.S. Schwartz (2003). "Implementing a Stochastic Model for Oil Futures Prices." *Energy Economics* 25(3): 215–238. [https://doi.org/10.1016/S0140-9883\(02\)00096-8](https://doi.org/10.1016/S0140-9883(02)00096-8).
- Culbertson, J. (1957). "The Term Structure of Interest Rates." *Quarterly Journal of Economics* 71(4): 485–517. <https://doi.org/10.2307/1885708>.
- D'Amico, S. and T.B. King (2013). "Flow and Stock Effects of Large-Scale Treasury Purchases: Evidence on the Importance of Local Supply." *Journal of Financial Economics* 108(2): 425–448. <https://doi.org/10.1016/j.jfineco.2012.11.007>.
- Diebold F.X., L. Liu, and K. Yilmaz (2018). "Commodity Connectedness." *Monetary Policy and Global Spillovers: Mechanisms, Effects and Policy Measures*, E. Mendoza, E. Pasten and D. Saravia Eds., Central Bank of Chile Press, Chile.
- Dimpfl, T. and F.J. Peter (2014). "The Impact of the Financial Crisis on Transatlantic Information Flows: An Intraday Analysis." *Journal of International Financial Markets, Institutions and Money* 31: 1–13. <https://doi.org/10.1016/j.intfin.2014.03.004>.
- Ederington, L.H., C.S. Fernando, K.V. Holland and T.K. Lee (2012). "Financial Trading, Spot Oil Prices, and Inventory: Evidence from the U.S. Crude Oil Market." *Price Working Paper*, University of Oklahoma, March.
- Fattouh, B. (2010). "The Dynamics of Crude Oil Price Differentials." *Energy Economics* 32(2): 334–342. <https://doi.org/10.1016/j.eneco.2009.06.007>.
- Favero, C.A. and F. Giavazzi (2002). "Is the International Propagation of Financial Shocks Non-linear? Evidence from the ERM" *Journal of International Economics* 57: 231–246. [https://doi.org/10.1016/S0022-1996\(01\)00139-8](https://doi.org/10.1016/S0022-1996(01)00139-8).
- Garbade, K.D. and W.L. Silber (1983). "Price Movements and Price Discovery in Futures and Cash Markets." *Review of Economics and Statistics* 65(2): 289–297. <https://doi.org/10.2307/1924495>.
- Garcia, P., S.H. Irwin and A.D. Smith (2015). "Futures Market Failure?" *American Journal of Agricultural Economics* 67(1): 40–64. <https://doi.org/10.1093/ajae/aau067>.
- Granger, C.W.J. (1969). "Investigating Causal Relations by Econometric Models and Cross-spectral Methods." *Econometrica* 37(3): 424–438. <https://doi.org/10.2307/1912791>.
- Gürkaynak, R.S. and J.H. Wright (2012). "Macroeconomics and the Term Structure" *Journal of Economic Literature* 50(2): 331–367. <https://doi.org/10.1257/jel.50.2.331>.
- Haigh, M.S. and D.A. Bessler (2004). "Causality and Price Discovery: An Application of Directed Acyclic Graphs." *Journal of Business* 74(4): 1099–1121. <https://doi.org/10.1086/422632>.

- Haigh, M.S., N.K. Nomikos and D.A. Bessler (2004). "Integration and Causality in International Freight Markets: Modeling with Error Correction and Directed Acyclic Graphs." *Southern Economic Journal* 71(1): 145–162. <https://doi.org/10.2307/4135317>.
- Hong, H. (2000). "A Model of Returns and Trading in Futures Markets." *Journal of Finance*. 55(2): 959–988. <https://doi.org/10.1111/0022-1082.00233>.
- Jaeck, E. and D. Lautier (2016). "Volatility in Electricity Derivative Markets: The Samuelson Effect Revisited." *Energy Economics* 59: 300–313. <https://doi.org/10.1016/j.eneco.2016.08.009>.
- Kawamoto, K. and S. Hamori (2011). "Market Efficiency among Futures with Different Maturities: Evidence from the Crude Oil Futures Market." *Journal of Futures Markets* 31(5): 487–501. <https://doi.org/10.1002/fut.20479>.
- Kogan, L., D. Livdan and A. Yaron (2009). "Oil Futures Prices in a Production Economy with Investment Constraints." *Journal of Finance* 64(3): 1345–1375. <https://doi.org/10.1111/j.1540-6261.2009.01466.x>.
- Lautier, D. (2005). "Segmentation in the Crude Oil Term Structure" *Quarterly Journal of Finance* 9(4): 1003–1020.
- Lautier, D. and F. Raynaud (2011). "Statistical Properties of Derivatives: A Journey in Term Structures." *Physica A* 390: 2009–2019. <https://doi.org/10.1016/j.physa.2011.01.018>.
- Lautier, D. and F. Raynaud (2012). "Systemic Risk in Energy Derivatives Markets: A Graph Theory Analysis." *Energy Journal* 9(4): 1003–1020.
- Liu, P. (P.) and K. Tang (2010). "No-Arbitrage Conditions for Storable Commodities and the Modeling of Futures Term Structures." *Journal of Banking and Finance* 34(7): 1675–1687. <https://doi.org/10.1016/j.jbankfin.2010.03.013>.
- Marschinski, R. and H. Kantz (2002). "Analysing the Information Flow between Financial Time Series—An Improved Estimator for Transfer Entropy." *European Physics Journal B* 30(2): 275–281. <https://doi.org/10.1140/epjb/e2002-00379-2>.
- Modigliani, F. and R. Sutch (1966). "Innovations in Interest Rate Policy." *American Economic Review* 56(1/2): 178–197.
- Onnela, J.-P. (2003). "Dynamic Asset Trees and Black Monday." *Physica A* 324: 247–252. [https://doi.org/10.1016/S0378-4371\(02\)01882-4](https://doi.org/10.1016/S0378-4371(02)01882-4).
- Pirrong, C. (2010). "An Evaluation of the Performance of Oil Price Benchmarks during the Financial Crisis." *Bauer College of Business Working Paper*, University of Houston, January.
- Rigobon, R. (2017). "Contagion, Spillover and Interdependence." *ECB Working Paper*, No. 1975, February.
- Robe, M.A. and J. Wallen (2016). "Fundamentals, Derivatives Market Information and Oil Market Volatility." *Journal of Futures Markets* 36(4): 317–344. <https://doi.org/10.1002/fut.21732>.
- Routledge, B.R., D.J. Seppi, and C.S. Spatt (2000). "Equilibrium Forward Curves for Commodities." *Journal of Finance* 55(3): 1297–1338. <https://doi.org/10.1111/0022-1082.00248>.
- Samuelson, P.A. (1965). "Proof that Properly Anticipated Prices Fluctuate Randomly." *Industrial Management Review* 6(2): 41–49.
- Schreiber, T. (2000). "Measuring Information Transfer." *Physical Review Letters* 85(2): 461–464. <https://doi.org/10.1103/PhysRevLett.85.461>.
- Schwartz, E. (1997). "The Stochastic Behavior of Commodity Prices: Implications for Valuation and Hedging." *Journal of Finance* 52(3): 923–973. <https://doi.org/10.1111/j.1540-6261.1997.tb02721.x>.
- Shannon, C.E. (1948). "A Mathematical Theory of Communication," *Bell System Technical Journal* 27(3): 379–423. <https://doi.org/10.1002/j.1538-7305.1948.tb01338.x>.
- Shannon, C.E. and W. Weaver (1949). *The Mathematical Theory of Information*. University of Illinois Press, Urbana, IL.
- Silvapulle, P. and I.A. Moosa (1999). "The Relationship Between Spot and Futures Prices: Evidence from the Crude Oil Market." *Journal of Futures Markets* 19(2): 175–193. [https://doi.org/10.1002/\(SICI\)1096-9934\(199904\)19:2<175::AID-FUT3>3.0.CO;2-H](https://doi.org/10.1002/(SICI)1096-9934(199904)19:2<175::AID-FUT3>3.0.CO;2-H).
- Singleton, K.J. (2014). "Investor Flows and the 2008 Boom/Bust in Oil Prices." *Management Science* 60(2): 300–318. <https://doi.org/10.1287/mnsc.2013.1756>.
- Smith, J.L., R. Thompson, and T.K. Lee (2015). "The Informational Role of Spot Prices and Inventories." *Journal of Energy Markets* 8(3): 95–121. <https://doi.org/10.21314/JEM.2015.124>.
- Sockin, M. and W. Xiong (2015). "Informational Frictions and Commodity Markets." *Journal of Finance* 70(5): 2063–2098. <https://doi.org/10.1111/jofi.12261>.
- Stein, J.C. (1987). "Informational Externalities and Welfare-reducing Speculation," *Journal of Political Economy* 95(6): 1123–1145. <https://doi.org/10.1086/261508>.
- Switzer, L.N. and M. El-Khoury (2007). "Extreme Volatility, Speculative Efficiency, and the Hedging Effectiveness of the Oil Futures Markets," *Journal of Futures Markets* 27(1): 61–84. <https://doi.org/10.1002/fut.20235>.
- Wang, Z. (2010). "Dynamics and Causality in Industry-Specific Volatility." *Journal of Banking and Finance* 34(7): 1688–1699. <https://doi.org/10.1016/j.jbankfin.2010.03.014>.



Connect with  
**IAEE**  
on facebook

